Marc Schitter, BSc

Drawdown scenarios for dams considering different states of saturation

MASTER'S THESIS

to achieve the university degree of

Diplom-Ingenieur

Master's degree programme: Geotechnical and Hydraulic Engineering

submitted to

Graz University of Technology

Supervisor

Ao.Univ.-Prof. Dipl.-Ing. Dr.techn. M.Sc. tit.Univ.-Prof. Helmut Schweiger

Dipl.-Ing. Georg Michael Ausweger, BSc

Institute of Soil Mechanics and Foundation Engineering

Graz, September 2017

Eidesstattliche Erklärung

Ich erkläre an Eides statt, dass ich die vorliegende Arbeit selbstständig verfasst, andere als die angegebenen Quellen/Hilfsmittel nicht benutzt, und die den benutzten Quellen wörtlich und inhaltlich entnommenen Stellen als solche kenntlich gemacht habe.

Graz, am …… ……

(Unterschrift)

Statutory declaration

I declare that I have authored this thesis independently, that I have not used other than the declared sources / resources, and that I have explicitly marked all material which has been quoted either literally or by content from the used sources.

Graz, …… ……

(signature)

Preface of the author

Da in der Hektik des Alltags oft vergessen wird ein Dankeschön auszusprechen, möchte ich mich bei dieser Gelegenheit ganz besonders bei meinen Eltern bedanken, die mich auch in steinigen Zeiten stets ermutigt und motiviert haben. Ohne Eure Unterstützung und Eurem Ansporn, wäre dieses Studium so nicht möglich gewesen. Danke für alles.

Da das Leben ohne Freunde auch nicht so ausgeglichen wäre, möchte ich mich an dieser Stelle auch bei all meinen Freunden die mich durch mein Leben und durch mein Studium begleitet haben, herzlich bedanken. Auch meiner Freundin möchte ich hiermit Danke für den stetigen Antrieb sagen.

Schließlich möchte ich mich auch noch bei meinen Betreuern, Herrn Dipl.-Ing. Dr.techn. Prof. Helmut Schweiger und ganz besonders bei Herrn Dipl.-Ing. Georg Ausweger für die hervorragende Betreuung bedanken, ohne die diese Arbeit nicht in diesem Stil gelungen wäre und der für jedes aufgetretene Problem in kurzer Zeit die richtige Lösung fand. Danke für diese lehrreiche Zeit.

Kurzfassung

Bei der Beurteilung der Damm- und Böschungsstabilität stellt die rasche Änderung des Wasserspiegels einen maßgebenden und wiederkehrenden Lastfall dar. Sei es durch die Sunkwirkung in Schifffahrtsstraßen oder durch Absenken der Stauspiegelhöhe in Staubecken. In der klassischen Bodenmechanik, in der der Boden unter dem Wasserspiegel als voll gesättigt (mit inkompressiblem Wasser) angenommen wird, bewirkt eine Änderung der totalen Spannungen, aufgrund hydraulischer Laständerungen oberhalb der horizontalen Geländeoberkante, keine Verformungen und Porenwasserüberdrücke. Wenn man aber nun davon ausgeht, dass der Boden erst ab einer gewissen Tiefe vollständig gesättigt ist, und sich somit unter dem Wasserspiegel noch Lufteinschlüsse befinden, können Verformungen auch durch hydraulische Laständerungen auftreten. Dies geschieht aufgrund der Lastverteilung zwischen den Bodenkörnern und dem Gas-Wasser Gemisch (Porenfluid). Ist das Gas-Wasser Gemisch aufgrund der Lufteinschlüsse kompressibel, werden des Weiteren auch die Porenwasserdrücke beeinflusst und Überdrücke entstehen im Falle einer hydraulischen Be- / Entlastung. Dies kann die Böschungsstabilität maßgebend beeinflussen und zu einem Versagen oder Abrutschen der Böschung führen. Ein Boden mit Luftblasen im Porenwasser wird als quasi-gesättigt bezeichnet.

Im Rahmen dieser Arbeit wird zuerst eine Vorstudie durchgeführt, um den Einfluss der Steifigkeit und Durchlässigkeit des Bodens im gesättigten und quasi-gesättigten Zustand auf die Porenwasserdruckentwicklung in einer Böschung während eines schnellen Abstaus zu zeigen. Dazu werden, unter Verwendung verschiedener Stoffmodelle, unterschiedliche Werte für die Steifigkeit und Durchlässigkeit untersucht. Anschließend wird ein reales Projekt unter Berücksichtigung verschiedener Sättigungszustände untersucht um die Einflüsse des Sättigungsgrads auf die Dammstabilität aufzuzeigen.

Abstract

For dams and slopes the rapid drawdown presents a crucial and recurring loading condition. A rapid change of the external water level, may result for example from a down surge in ship ways or from a drawdown in a water retention basin. In classical soil mechanics, where the soil beneath the phreatic level is assumed to be fully saturated (with incompressible water), a change in total stresses due to a water level change above a horizontal ground surface will cause no deformations and no excess pore water pressures. However, assuming that the soil is only fully saturated at a certain depth and therefore entrapped air bubbles are present below the phreatic level, deformations due to hydraulic loading can occur. This is caused by the load distribution between the soil skeleton and the air water mixture (pore fluid). The pore fluid is compressible when entrapped air is present. Due to this compressibility of the pore fluid the pore water pressure development is influenced and excess pore water pressures develop in case of hydraulic loading. This could lead to a significant decrease of the slope stability and therefore cause a failure of the slope or a landslide. Soils with entrapped air bubbles in the pore fluid are called quasi-saturated.

In the course of this thesis at first a preliminary study is performed to evaluate the influence of stiffness and permeability of the soil in a saturated and a quasi-saturated state on the development of pore water pressures in a slope during a rapid drawdown. Therefore various values for stiffness and permeability are evaluated, using different constitutive models. Subsequently a real project is analysed in terms of different saturation states to show their influence on slope stability.

Table of contents

List of figures

List of tables

List of symbols and abbreviations

Capital letters

A	[-]	Skempton pore pressure parameter
B	[-]	Skempton pore pressure parameter
$E´$	[kN/m²]	Young's modulus
E_0	[kN/m²]	Stiffness at very small strains
E_{50}	[kN/m²]	Stiffness in triaxial compression
E_{oed}	[kN/m²]	Stiffness in compression
E_s	[kN/m²]	Stiffness in compression
E_{ur}	[kN/m²]	Stiffness in un-/reloading
E_v	[kN/m²]	Deformation modulus of plate loading test
G_0	[kN/m²]	Shear modulus
H	[m]	Initial water level
H_D	[m]	Height of drawdown
K_0	[-]	Earth pressure at rest
K_{air}	[kN/m²]	Bulk modulus of air
K_w	[kN/m²]	Bulk modulus of water
K_{wg}	[kN/m²]	Bulk modulus of the pore fluid
S	[-]	Degree of saturation
$S(\phi)$	[-]	Suction head depending degree of saturation
S_{eff}	[-]	Effective degree of saturation
S_{pw}	[-]	Pressure depending degree of saturation
S_{res}	[-]	Residual degree of saturation
S_{sat}	[-]	Saturated degree of saturation
T	[-]	Dimensionless time factor
U	[-]	Degree of irregularity

Small letters

c	[kN/m²]	Cohesion
$c(U)$	[-]	Factor of correction
d_{10}	[mm]	10% sieve pass through
d_{60}	[mm]	60% sieve pass through
e_{init}	[-]	Initial void ratio
g_a	[1/m]	Fitting parameter for the air entry value of the soil
g_c	[-]	Fitting parameter to make two parameter equation
g_n	[-]	Fitting parameter for water extraction when air entry is exceeded

h	[-]	Henry parameter (equation 8)
h	[m]	Water level
k	[m/s]	Permeability
k_0	[m/s]	Permeability at boundary to unsaturated zone
k_{qs}	[m/s]	Quasi-saturated permeability
k^{rel}	[m/s]	Relative permeability
k^{sat}	[m/s]	Saturated permeability
k_{slope}	[m/s]	Permeability of the slope
$k_{subsoil}$	[m/s]	Permeability of the subsoil
k_{unsat}	[m/s]	Unsaturated permeability
k_x	[m/s]	Horizontal permeability
k_y	[m/s]	Vertical permeability
m	[-]	Power of stress dependency
n	[-]	Fitting parameter (equation 6)
n	[-]	Porosity of the soil
p	[kN/m²]	Total mean stress
p_a	[kN/m²]	Atmospheric pressure
p_{active}	[kN/m²]	Active pore water pressure
p_{excess}	[kN/m²]	Excess pore water pressure
p_{ref}	[kN/m²]	Reference pressure
p_{steady}	[kN/m²]	Steady state pore water pressure
p_{water}	[kN/m²]	Pore water pressure
q	[kN/m²]	Total deviatoric stress
t_{DD}	[s]	Drawdown time
v_{DD}	[m/s]	Drawdown velocity
Δh	[m]	Change in water level

Greek letters

φ	[°]	Friction angle of the soil
γ_{sat}	[kN/m³]	Wet unit weight of the soil
γ_w	[kN/m³]	Unit weight of water
ϕ	[m]	Suction Head
γ'	[kN/m³]	Effective unit weight of the soil
$\gamma_{0.7}$	[-]	Shear strains at 70% of G_0
γ_{unsat}	[kN/m³]	Dry unit weight of the soil
ν	[-]	Poisson's ratio

ν_{ur}	[-]	Poisson's ratio for un-/reloading
σ'	[kN/m²]	Effective stresses
σ^{tot}	[kN/m²]	Total stresses
ω	[m³]	Volumetric air content
ω_{max}	[m³]	Volumetric air content related to k_0
ψ	[°]	Dilatancy angle

Abbreviations

FE	Finite Element
HSS	Hardening Soil model with small strain stiffness
LE	Linear-elastic constitutive model
MC	Mohr-Coulomb constitutive model
SWCC	Soil water characteristic curve

1 Introduction

In classical soil mechanics a fully saturated state below phreatic level is assumed. This indicates that all pores are filled with water. However, a fully saturated state is usually not reached directly below the phreatic level as a small amount of entrapped air stays in the water. Therefore, a fully saturated state is not reached until a certain depth depending on the prevailing soil. The assumption considered by classical soil mechanics may be sufficient for most cases, but for certain load cases the amount of entrapped air has to be taken into account.

Considering a fully saturated state and thereby a two phase medium soil (consisting of soil grains and assumed incompressible water) can lead to misjudgement of the soil behaviour. This could especially be the case for a change in total stresses due to changes in water level resulting from drawdowns or other fast changes of the external water level. In case of full saturation and 1D conditions, pore water pressures change simultaneously with changing external water levels. This is not the case for quasi-saturated soils (pore fluid with entrapped air bubbles).

An amount of entrapped air and therefore a degree of saturation smaller than 1 leads to a different load distribution between air water mixture and soil grains. Skempton (1954) describes this load distribution for undrained soils with his pore pressure coefficients *A* and *B*.

This thesis is about the investigation of pore water pressure development for drawdown scenarios considering different state of saturation numerically with the program Plaxis2D 2016 (Brinkgreve 2016).

In a first step the pore water pressure development is investigated for a simple slope with different constitutive models, to evaluate the influence of stiffness under fully saturated and quasi-saturated conditions. In a further step a real project is analysed concerning pore water pressure development and slope stability according to different saturation states.

The purpose of this thesis is to show the influence of a quasi-saturated soil on pore water pressure development and resulting excess pore water pressures and thereof the influence on slope stability for drawdown conditions.

2 Short introduction to drawdown conditions

Drawdown conditions are defined by a temporal change of the water level at the upstream side of a dam. If the rate of lowering the water level is high compared to the permeability of the soil, $v_{DD} \geq k$, it is characterized as a rapid drawdown (Muth et al, 2001).

In history two basic approaches are described to analyse a drawdown based on the behaviour of the available material. In addition to the undrained analysis and the flow analysis a fully coupled flow deformation analysis can be performed (Alonso & Pinyol 2009). Latter leads to the most realistic results, whereas the flow only analysis usually does not result in correct pore water pressures (Alonso & Pinyol 2009). For materials with low permeability also an undrained analysis might give right results.

The concept of a drawdown (see Fig. 1) is described by its initial conditions which are given by the height of the water level H acting on the slope. The external water level is lowered to a height of $H - H_D$ over a time t_{DD}. This leads to a change in total stresses (stabilizing effect of the water pressure) as well as a change in the hydraulic boundary conditions due to the reduction of the external water level (Alonso & Pinyol 2009). According to the changes in total stresses the initial hydrostatic pore water pressure acting on the slope and surface (Fig. 1a) changes to the lowered state (Fig. 1b). The resulting stress relaxation is shown in Fig. 1c. Furthermore the new hydrostatic pore water pressure is given with $p_w = (H - H_D)\,\gamma_w$. Due to the change in the hydraulic pressure on the slope also the total stresses inside the slope change. This effect leads to excess pore water pressures. These excess pore water pressures result in an additional hydraulic gradient and a flow regime develops. Considering drained conditions with a high permeability of the soil the excess pore water pressures may dissipate fast, but with a low permeability of the soil, the generated pore pressures can cause serious damages or even a failure of the dam. (Alonso & Pinyol 2009)

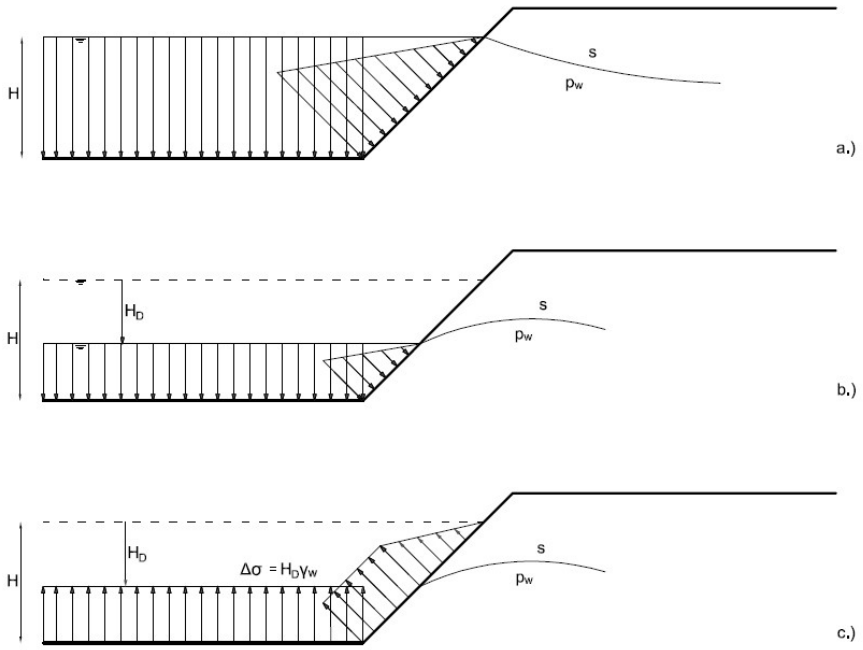

Fig. 1 Principle of a drawdown (from Alonso & Pinyol 2009)

3 Introduction in quasi-saturated soils

Generally, the water conditions in soils can be divided into four stages of saturation, depending on the amount of air. Unsaturated soil mechanics describes the soil as a three-phase medium consisting of soil grains, water and air. The mixture of water and air is called pore fluid. In case of full saturation the pore fluid is generally assumed as nearly incompressible. Already a small amount of entrapped air however, leads to a significant increase of the pore fluid compressibility.

Figure 2 shows the stages of saturation. If all pores are completely filled with water the soil is called fully saturated. When a small amount of entrapped air bubbles is present the soil is no longer fully saturated but the air phase is still discontinuous. In this state the soil is described as quasi-saturated. The degree of saturation is slightly below 1. In case of a continuous air phase which only occurs above the phreatic level, the soil is called unsaturated.

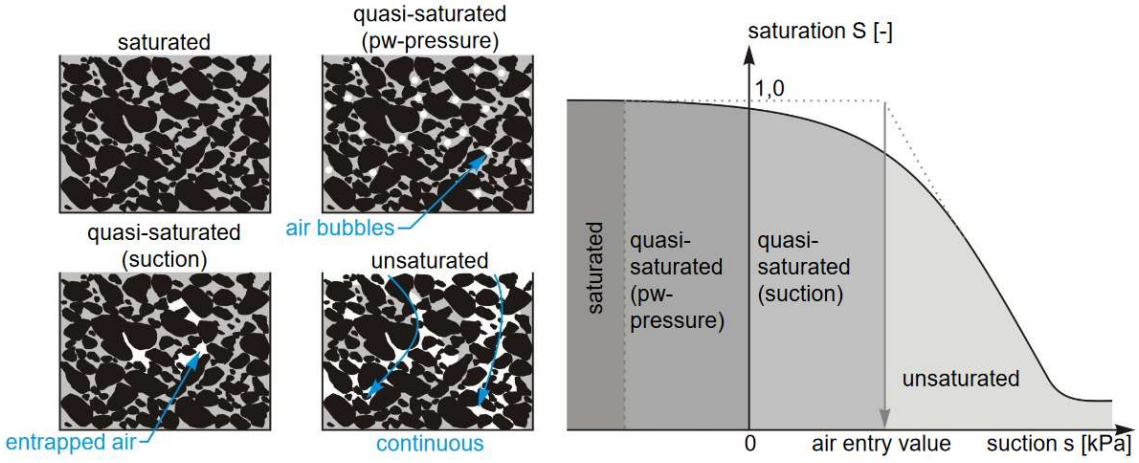

Fig. 2 Stages of saturation (from Boutonnier 2010)

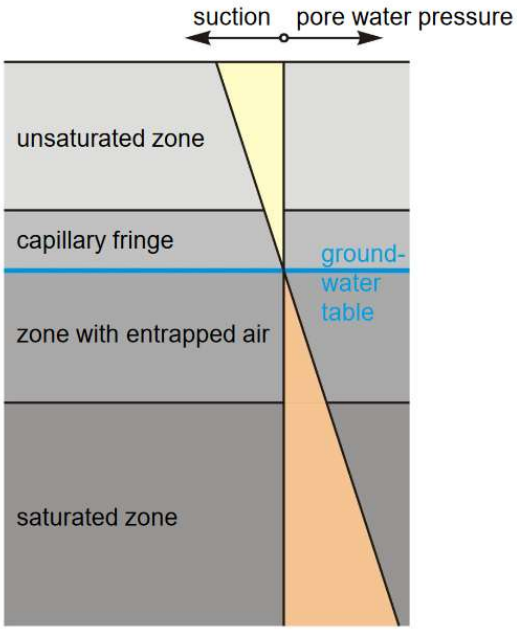

Fig. 3 Regions of a soil segment (from Köhler & Montenegro 2005)

The term quasi-saturated can be applied to an area above and below, but in vicinity of the phreatic level. It describes the transition zones between unsaturated, where the current suction is lower than the air entry value, and saturated zone. The capillary fringe is the quasi-saturated zone above the phreatic level and indicates suction. Suction is defined by negative pore water pressure and results from the capillary tension within the soil. The zone with entrapped air is the quasi-saturated zone below the phreatic level. This zone contains a continuous water phase and air bubbles. These air bubbles get more and more dissolved by getting far enough from the phreatic level (saturated zone). (Köhler & Montenegro 2005)

Quasi-saturation in soils can develop due to several reasons:

- Change of the present ground water table due to the infiltration of rainfall or flood events
- In dams during drawdown events or fluctuating water levels
- Increase of air content due to increase in temperature or decomposition of organic parts (Faybishenko 1995)

The resulting increase of the pore fluid compressibility effects the pore water pressure development as well as deformations. In fully saturated soils deformations are the result of mechanical loading (hydraulic loading above ground surface will not produce any deformations). When the soil permeability is low, all the load is transferred only to the

water (incompressible, no volumetric changes). The resulting excess pore water pressure will dissipate with time and deformations occur as the load distribution changes.

In quasi-saturated soils deformations can occur due to mechanical and hydraulic loading. Due to the entrapped air water will flow into the quasi-saturated zone in case of an increase of the present water level. This will behave like a change in loading and deformations are the result. For mechanical loading the load is not transferred only to the water, it is distributed between the water and the soil due to the entrapped air. The amount of the load distribution is depending on the soil stiffness as well as on the bulk modulus of the pore fluid. (Skempton 1954; Montenegro et al 2015).

Skempton (1954) determines the distribution of the applied external load between soil grains (change of effective stresses) and pore fluid (change of pore water pressure) with his dimensionless factor *B*. If an external load is applied the *B* parameter can be used to describe the change of pore water pressure for both, uniaxial and isotropic loading.

$$\Delta p_{water} = B * \Delta \sigma^{tot} \quad (1)$$

Δp_{water}	[kN/m²]	change in pore water pressure
B	[-]	Skempton *B* parameter
$\Delta \sigma^{tot}$	[m]	Change in total stresses

The B-parameter and therefore the magnitude of pore water pressure changes are mostly depending on the governing parameters of the soil stiffness and the bulk modulus of the pore fluid under consideration of the porosity (Montenegro et al 2015).

$$B = \frac{1}{1 + n * \frac{E_s}{K_{wg}}} \quad (2)$$

B	[-]	Skempton *B* parameter for oedometric loading
n	[-]	Porosity of the soil
E_s	[kN/m²]	Oedometer modulus of the soil
K_{wg}	[kN/m²]	Bulk modulus of the pore fluid

The bulk modulus of the pore fluid K_{wg} is composed of the bulk modulus of water K_w and the bulk modulus of air K_{air} and is depending on the degree of saturation. Therefore, the *B* parameter depends on the degree of saturation as well (Montenegro et al 2015).

$$K_{wg} = \frac{S}{K_w} + \frac{(1-S)}{K_{air}} \quad (3)$$

S	[-]	Degree of saturation
K_w	[kN/m²]	Bulk modulus of water
K_{air}	[kN/m²]	Bulk modulus of air

Depending on the used parameters the value for *B* is in a range between 0 and 1. A value of B = 0 indicates a dry soil, load changes have no effects on the pore water pressure. For a fully saturated soil B = 1 as the pore fluid is incompressible. External load changes will have an effect on the pore water pressure. This change in pore water pressure is equal to the change in total stresses. (Montenegro et al 2015)

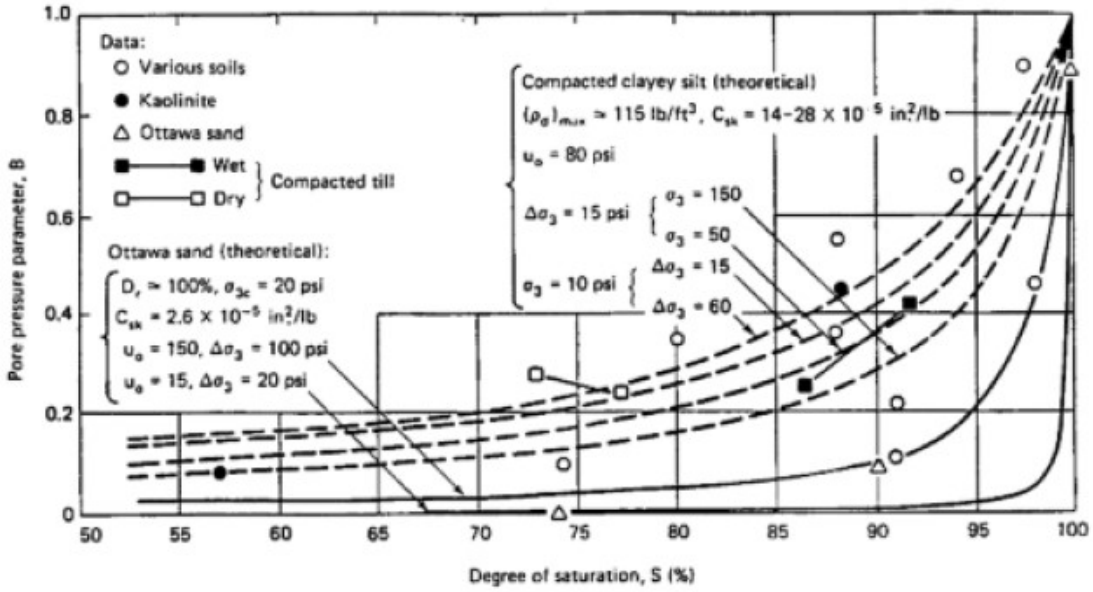

Fig. 4 Connection between *B* parameter and saturation (Black & Lee 1973)

Using the Skempton parameter to evaluate the change in pore water pressure due to hydraulic loading or unloading (raising or lowering the water table above the ground surface) instead of mechanical loading $\Delta\sigma$, is possible if $\Delta\sigma^{tot}$ is replaced by $\Delta h\gamma_w$.

$$\Delta p_{water} = B * \Delta\sigma^{tot} = B * \Delta h\gamma_w \quad (4)$$

Δh	[m]	Change of the water level
γ_w	[kN/m²]	Unit weight of water

Applying equation (4) in case of a quasi-saturated soil, the change in pore water pressure is not equal to the hydrostatic water pressure change due to the hydraulic loading, as it would be the case for a fully saturated soil. For hydraulic unloading ($\Delta h < 1$) excess pore

water pressure will be the result as the complement of (B-1) acts like an additional surcharge. According to Montenegro et al (2015) this excess pore water pressure can be calculated with

$$p_{excess} = (B - 1) * \Delta h \gamma_w \quad (5)$$

p_{excess} [kN/m²] Resulting excess pore water pressure

Due to the entrapped air in the pores the permeability of the soil is decreased. Based on laboratory tests Faybishenko (1995) presented an equation for the quasi-saturated permeability as a function of the volumetric air content.

$$k^{qs} = k_0 + (k^{sat} - k_0) * (1 - \frac{\omega}{\omega_{max}})^n \quad (6)$$

k^{qs}	[m/s]	Quasi-saturated permeability
k_0	[m/s]	Permeability at the boundary between quasi-saturated and unsaturated zone
k^{sat}	[m/s]	Saturated permeability
ω	[m³]	Volumetric air content
ω_{max}	[m³]	Volumetric air content which is related to k_0
n	[-]	Fitting parameter

A simplified equation for the unsaturated (quasi-saturated) permeability is the following. (Alonso & Pinyol 2009)

$$k^{unsat} = k^{sat} * S^3 \quad (7)$$

k^{unsat} [m/s] Unsaturated permeability

According to Boyle's law the entrapped air bubbles in the pore fluid get compressed in case of an increase of the pore fluid pressure. Thereof the degree of saturation as well as the pore fluid compressibility (see equation (3)) depend on the pore fluid pressure. Based on Boyle's law and Henry's law the following relation between the pore fluid pressure and pore fluid compressibility can be derived. (Boutonnier 2010)

$$S_{pw} = \frac{1}{1 - h + \frac{p_a}{p_w + p_a} * \frac{S_{pw=} * (h-1) + 1}{S_{pw=0}}} \quad (8)$$

S_{pw}	[-]	Pressure depending degree of saturation
$S_{pw=0}$	[-]	Saturation at $p_w = 0$
h	[-]	Henry parameter (usually 0.02)
p_a	[kN/m²]	Atmospheric pressure
p_w	[kN/m²]	Pore water pressure

4 Preliminary study

In the current preliminary study a simple slope, which is shown in Fig. 5, is used to investigate and compare the pore water pressure development for rapid and slow drawdown conditions. The calculations are executed with the finite element program Plaxis2D 2016 (Brinkgreve 2016).

In the first part of the study a linear-elastic constitutive model is applied with different stiffnesses to determine the influence of the stiffness on the magnitude of the pore water pressure. Therefore three different stiffnesses are chosen to represent a primary loading, an un-/reloading and a stiffness at small strains of a soft soil. The primary loading stiffness in compression E_{oed}, the un-/reloading stiffness E_{ur} and the stiffness at small strains E_0 are converted to the Young's modulus E' as input parameter for the linear-elastic constitutive model. The same values for the stiffnesses are also used later for calculations with other constitutive models like the Mohr-Coulomb model and the Hardening Soil model with small strain stiffness.

Second part of the preliminary study comprise analysis with the linear-elastic perfectly-plastic Mohr-Coulomb and with the elastoplastic Hardening Soil model with small strain stiffness. In this part the influences of soil permeability and constitutive model are shown.

In selected calculations the quasi-saturated state is considered by assuming a constant bulk modulus of the pore fluid of K_{wg} = 10 000 kN/m² to investigate the influence of a compressible pore fluid. According to equations (3) and (8) the chosen pore fluid bulk modulus corresponds roughly to a content of entrapped air of 3%. Furthermore a soil water characteristic curve (including the quasi-saturated range) is introduced for the Mohr-Coulomb constitutive model which describes the influence of the degree of saturation on the permeability (SWCC described in chapter 4.4).

4.1 Geometry, constitutive models and setup

The slope, which is used for this preliminary study has a height of 10 m and a horizontal length of 27.47 m leading to an inclination of 20°. The pore water pressure is evaluated in four nodes. One is near the right boundary of the model (node A), one is beneath the end of the slope (node B) and two nodes are within the slope itself (nodes C and D). The initial ground water table is defined horizontally at 1 m below slope crest. Fig. 5 shows the exact geometry with 3,146 15-noded elements.

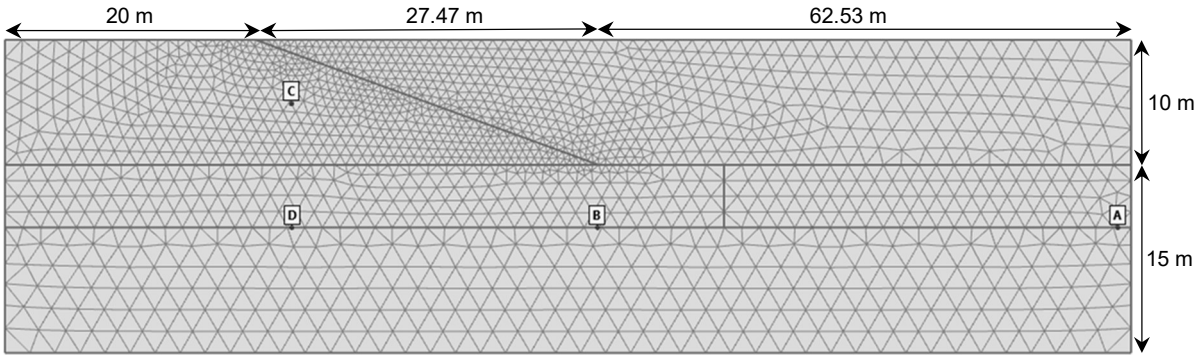

Fig. 5 Geometry of the simple slope with the four nodes

The hydraulic boundary conditions on the left, right and lower limit are assumed to be impermeable.

For the calculations three different constitutive models are used to describe the soil:

- **Linear-elastic model**

  Although the linear-elastic model is not accurate to model the non-linear behaviour of soil and is rather used to model structural behaviour, it is well suited for basic investigations due to its relatively simple behaviour. No stress dependency of the soil stiffness or plasticity are considered. There is also no coupling between shear and volumetric behaviour. This model only uses two input parameters based on Hooke's law; the Young's modulus E' and the Poisson's ratio ν. Strength parameters (friction angle φ, cohesion c and dilatancy angle ψ) cannot be entered (Brinkgreve 2016).

- **Mohr-Coulomb model**

  Stress dependency may also not be considered with the linear-elastic perfectly-plastic Mohr-Coulomb model but it considers plasticity and the Mohr-Coulomb failure criteria, which makes it recommendable for a first estimation. Strength parameters are the friction angle φ, the cohesion c and the dilatancy angle ψ.

- **Hardening soil model with small strain stiffness**

  This advanced model considers the stress dependency of the soil with the ratio of stress dependency m. In addition to a stress dependent stiffness a different stiffness for primary loading and un-/reloading is used. Furthermore an increased stiffness at small strain level is considered with the initial shear modulus G_0 and the shear strains at 70% of G_0 $\gamma_{0.7}$ to describe the variation of stiffness with strain. (Brinkgreve 2016).

The used soil parameters for the three different models can be seen in the following tables.

Tab. 1 General parameters

	All models		
Parameter	**Abbreviation**	**Value**	**Unit**
Unsaturated unit weight	γ_{unsat}	19	[kN/m³]
Saturated unit weight	γ_{sat}	20	[kN/m³]
Groundwater			
Data Set	-	Hypres	[-]
Model	-	Van Genuchten	[-]
Permeabilities	k_x / k_y	1E-7 1E-4 1E-3	m/s
Initial			
K_0 Determination	K_0	Automatic	[-]

Tab. 2 Model specific parameters for linear-elastic model

	Linear-elastic		
Parameter	**Abbreviation**	**Value**	**Unit**
Material model	-	linear-elastic	[-]
Drainage type	-	Drained	[-]
Parameters			
Young's modulus	E´	10 120 25 310 101 200	[kN/m²]
Poisson's ratio	ν	0.33	[-]

Tab. 3 Model specific parameters for Mohr-Coulomb model

	Mohr-Coulomb		
Parameter	**Abbreviation**	**Value**	**Unit**
Material model	-	Mohr-Coulomb	[-]
Drainage type	-	Drained	[-]
Parameters			
Young's modulus	E´	10 120	[kN/m²]
Poisson's ratio	ν	0.33	[-]
Cohesion	c	3/6.5*	[kN/m²]
Friction angle	φ	34.5/38.5*	[°]
Dilatancy angle	ψ	0	[°]

Tab. 4 Model specific parameters for Hardening Soil Small model

	Hardening Soil Small model		
Parameter	**Abbreviation**	**Value**	**Unit**
Material model	-	HS small	[-]
Drainage type	-	Drained	[-]
Parameters			
Triaxial stiffness	E_{50}	18 000	[kN/m²]
Oedometer stiffness	E_{oed}	15 000	[kN/m²]
Un-/reloading stiffness	E_{ur}	37 500	[kN/m²]
Power of stress dependency	m	0.7	[-]
Cohesion	c	3/6.5*	[kN/m²]
Friction angle	φ	34.5/38.5*	[°]
Dilatancy angle	ψ	0	[°]
Small strain shear modulus	G_0	62 500	[kN/m²]
Shear strains at 70% of G_0	$\gamma_{0.7}$	0.0001	[-]
Poisson's ratio for un-/reloading	ν_{ur}	0.2	[-]

* For fully saturated/quasi-saturated respectively

To investigate the influence of soil permeability on the pore water pressure development, three different values are analysed: k = 1E-7 m/s and k = 1E-4 m/s. For the third variation the permeabilities of the slope and the subsoil are different. For the slope k = 1E-3 m/s and for the subsoil k = 1E-7 m/s is assumed. (see Tab. 1).

The FE – calculation is performed with the following phases. In the initial phase a K_0-Procedure is performed. The subsequent "Excavation" phase is performed as a plastic calculation (drained). After the excavation two different drawdown phases are introduced as a fully coupled flow deformation analysis. One where the water level is lowered 7 m within a time of 8 hours (corresponds to 0.33 days) and one where the water level is lowered 7 m within 7 days. This leads to drawdown rates of 0.875 m/h and 1 m/day respectively. To apply the drawdown rates to the geometric model it is necessary to define two different hydraulic head functions in the program Plaxis2D 2016. The two head functions are defined as linear functions where the groundwater level is lowered -7 m in the respective time.

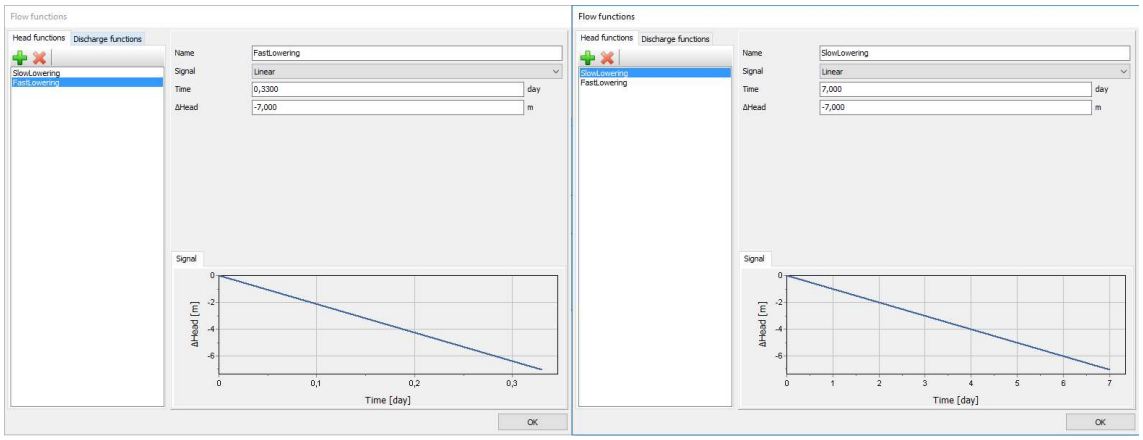

Fig. 6 Defined head functions

The drawdown phases are followed by a consolidation phase which is also performed as a fully coupled flow deformation analysis with a very high time period (1500 days) and a constant lowered water level.

4.2 Pore water pressures in Plaxis2D

For a better understanding the pore water pressure definition in Plaxis2D 2016 is presented briefly in the following. Pressures in Plaxis2D 2016 are defined negative and suction is defined positive. The active pore water pressure p_{active} is defined by the effective saturation S_{eff} and the pore water pressure p_{water}.

$$p_{active} = S_{eff} * p_{water} \quad (9)$$

p_{active}	[kN/m²]	Active pore water pressure
p_{water}	[kN/m²]	Pore water pressure
S_{eff}	[-]	Effective degree of saturation

Considering fully saturated conditions the active pore water pressure is equal to the pore water pressure p_{water} because the degree of saturation is 1. A difference occurs when partially saturated soil behaviour above the phreatic level is taken into account. In the case of quasi-saturated soil $p_{active} \approx p_{water}$ can be assumed, as the degree of saturation is nearly 1.

The pore water pressure is defined by the steady state pore water pressure p_{steady} and the excess pore water pressure p_{excess}. Using deformation analysis like plastic calculation or consolidation, p_{excess} results from soil behaviour and p_{water} is calculated with.

$$p_{water} = p_{steady} + p_{excess} \quad (10)$$

p_{steady}	[kN/m²]	Pore water pressure at steady state
p_{excess}	[kN/m²]	Excess pore water pressure

Considering a fully coupled flow deformation analysis, p_{steady} is calculated based on the steady state groundwater flow at the end of the calculation phase, p_{water} is calculated together with the displacements and p_{excess} can be back calculated.

$$p_{excess} = p_{water} - p_{steady} \quad (11)$$

The shown figures in this study are plotted with p_{water} as it is the result of the calculation. In general using fully coupled flow deformation analysis p_{water} should be plotted instead of p_{excess}. The excess pore water pressure can then be derived by considering the phreatic level of the calculation phase. (Brinkgreve 2016).

4.3 Linear-elastic calculation for evaluating stiffness influence

4.3.1 Introduction

In the following linear-elastic calculations are carried out with different stiffnesses to evaluate their influence on the pore water pressure development. Three different typical values are used for the Young's modulus which corresponds to the oedometer modulus, the un-/reloading stiffness and the small strain stiffness of a sandy silt. Due to the different definitions of the Young's modulus and typical soil stiffnesses (E_{oed}, E_{ur} and E_0),

the soil stiffness has to be converted into a corresponding Young's modulus. For the sake of simplicity, a loading under lateral confinement is assumed for all stiffness definitions. This is shown exemplarily for the oedometer modulus in Equation (12). Furthermore calculations considering quasi-saturation are carried out. In a simplified procedure a constant value for the bulk modulus of the pore fluid of K_{wg} = 10 000 kN/m² is assumed. This value leads to different values for the *B* parameter depending on the used stiffness.

$$E' = \frac{E_{oed} * (1 - 2\upsilon) * (1 + \upsilon)}{(1 - \upsilon)} = 10\,120\ [kN/m^2] \qquad (12)$$

E'	[kN/m²]	Young's modulus
E_{oed}	[kN/m²]	Oedometer stiffness
υ	[-]	Poisson's ratio (0.33 in this case)

This leads to the following B-coefficients.

$$B^{oed} = \frac{1}{1 + n * \frac{E'}{K_{wg}}} = 0.75 \qquad (13)$$

B^{oed}	[-]	Skempton *B* parameter for primary loading (E_{oed})
n	[-]	Porosity of the soil (0.33 in Plaxis2D 2016)
E´	[kN/m²]	Calculated Young's modulus for primary loading (E_{oed})
K_{wg}	[kN/m²]	Bulk modulus of the pore fluid (concerning boundary condition)

$$B^{ur} = \frac{1}{1 + n * \frac{E'}{K_{wg}}} = 0.55 \qquad (14)$$

B^{ur}	[-]	Skempton *B* parameter for un-/reloading
E´	[kN/m²]	Calculated Young's modulus for un-/reloading (E_{ur})

$$B^{sss} = \frac{1}{1 + n * \frac{E'}{K_{wg}}} = 0.23 \qquad (15)$$

B^{sss}	[-]	Skempton *B* parameter for small strain stiffness range
E´	[kN/m²]	Calculated Young's modulus for small strain range (E_0)

The value for the porosity *n* is 0.33 as in the program Plaxis2D 2016 the initial void ratio is by default e_{init} = 0.5.

4.3.2 Results of linear-elastic study

The results shown below in Fig. 7 represent the pore water pressure in node A during rapid drawdown (7 m/8 h). It can be seen that for calculations considering fully saturation (black, green and blue lines), the influence of the stiffness on the pore water pressure is negligible. The pore water pressure development is approximately equal to the hydrostatic pore water pressure change due to the full saturation (B ≈ 1). Furthermore the conditions at node A represent almost a 1D-loading (with no changes in deviatoric stress).

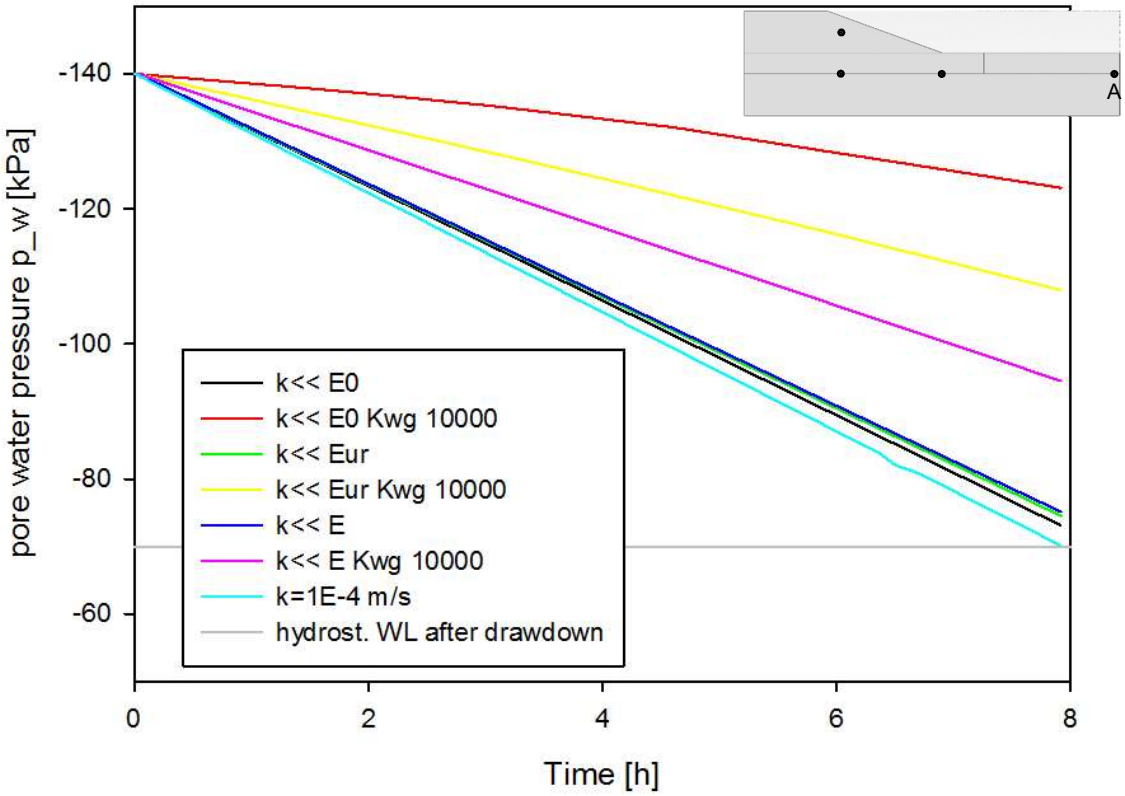

Fig. 7 Results for pore water pressure in node A

Also calculations with a permeability of k = 1E-4 m/s are carried out (light blue line). Due to the fact that the results are nearly identical, independent from the used stiffnesses and pore fluid bulk modulus they are represented by one line in Fig. 7. This results from the relatively high permeability which leads to dissipation of the high pore water pressures concurrently with the drawdown event.

Considering quasi-saturation with a bulk modulus of the pore fluid of K_{wg} = 10 000 kN/m², shows that the pore water pressures differ according to different stiffnesses (red, yellow and pink lines in Fig. 7), as it can be shown with Skempton's B-coefficient. For a highly stiff soil (small strain stiffness) the *B* value is small (about 0.23). 23% of the load change are transferred to the pore fluid. The remaining 77% of the load change are carried by

the soil skeleton. According to equation (5) the excess pore water pressure, due to drawdown, can be calculated with

$$p_{excess} = (0.23 - 1) * (-7) * 10 = 53.9\ kPa \quad (16)$$

If this value is compared with the difference between the hydrostatic pore water pressure after the drawdown (70 kPa) and the calculated pore water pressure (123.12 kPa), the results of the FE-analysis (Fig. 7) fit quite well with the before calculated excess pore water pressure. The same applies for the other stiffnesses.

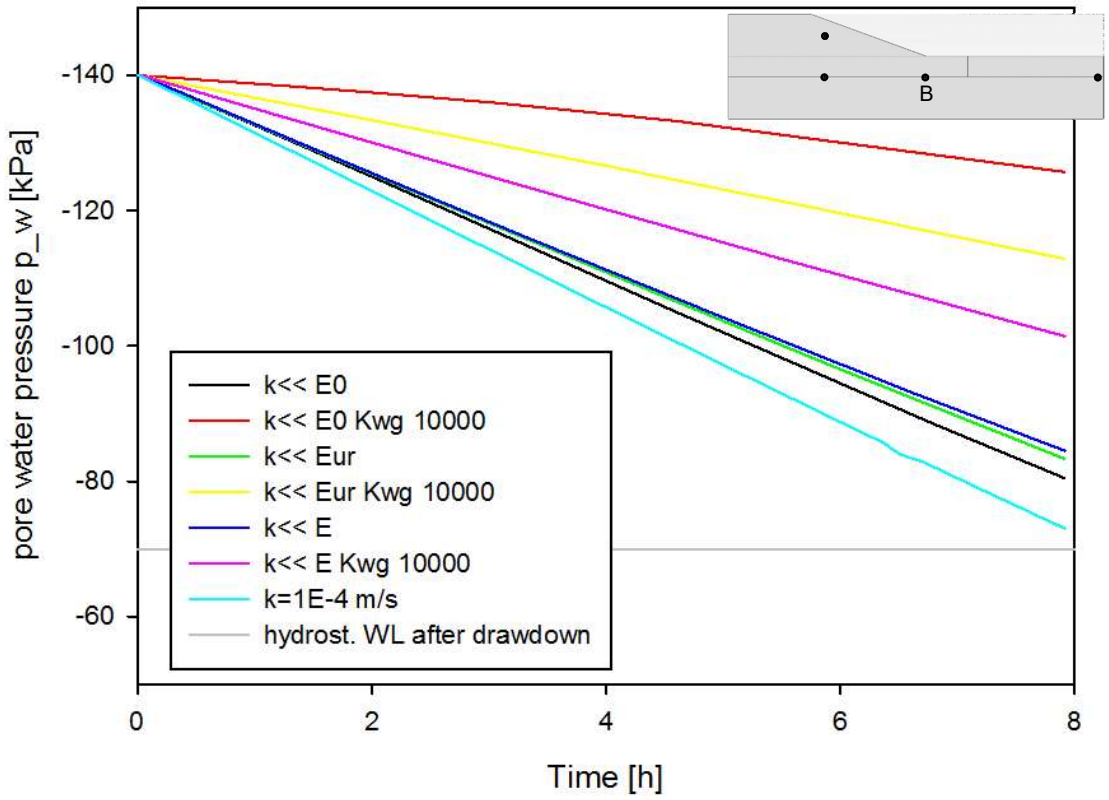

Fig. 8 Results for pore water pressure in node B

Node B, located beneath the slope end, shows a slight difference in the results in contrast to node A. In node B an excess pore water pressure is also produced in case of full saturation (see black, green and blue lines). However, the influence of the soil stiffness is still small. Pore water pressure in node B is influenced by the developing flow regime due to the disequilibrium of the water levels. The internal water level cannot be lowered as fast as the external one. This leads to a disequilibrium between those two and water starts flowing. Furthermore the pore water pressure in this area is influenced by the change in deviatoric stress which develops after the supporting water body is removed during drawdown.

Results for a soil with a permeability of k = 1E-4 m/s (see light blue line) reach the hydrostatic pore water pressure directly after the drawdown again independent from the used stiffnesses and bulk modulus of the pore fluid. Immediately resulting excess pore water pressures can dissipate simultaneously with drawdown.

As well as in node A the influence of quasi-saturation can be clearly seen. Due to the different stiffnesses and the constant value for K_{wg} = 10 000 kN/m² the *B* value differs. With this difference of the *B* value, the load change distribution changes as well. The results for excess pore water pressures after the drawdown are higher than those in node A. The reason for that was already explained before for fully saturated soil conditions. It can be seen that the amount of entrapped gas, influencing the compressibility of the pore fluid has a high influence on the developing pore water pressures. Excess pore water pressures can have a serious influence on the stability of a slope due to the fact that they reduce the effective stresses. Therefore, the high compressibility of the pore fluid, cannot be neglected in some cases. As already mentioned before, a constant pore fluid bulk modulus of K_{wg} = 10 000 kN/m² corresponds roughly to 3% entrapped air according to equation (3) and (8).

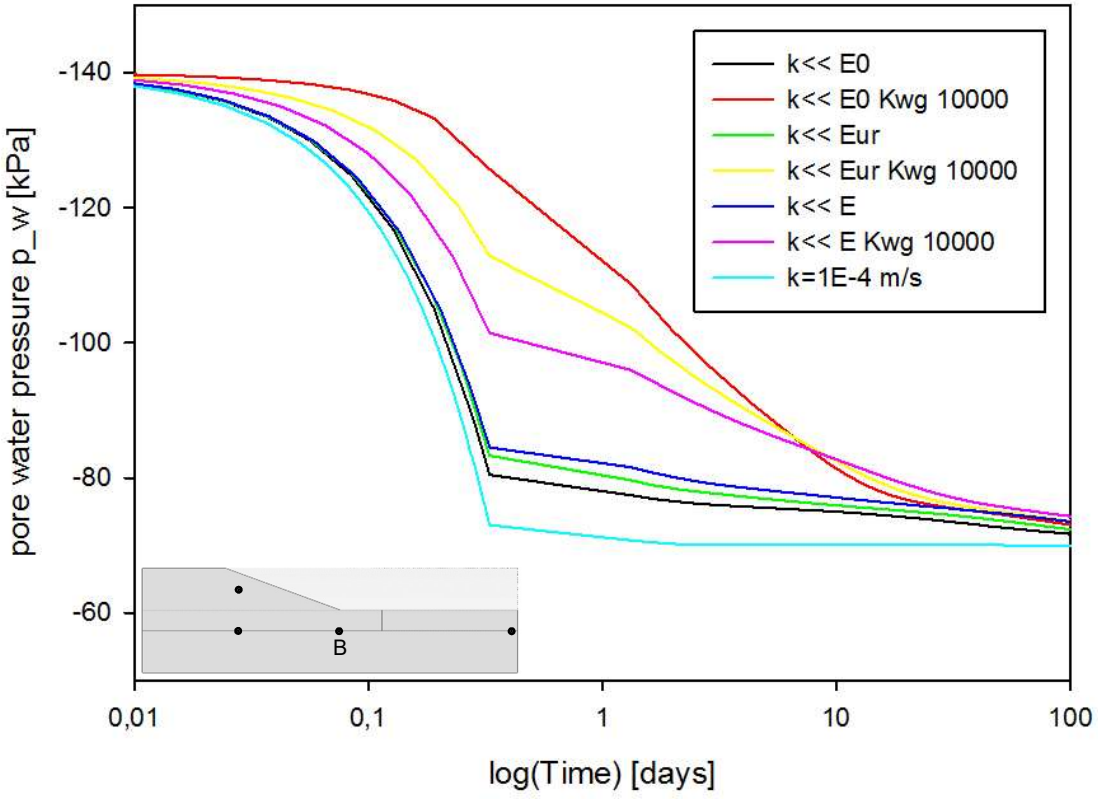

Fig. 9 Results for consolidation in node B

For completeness the results for the performed consolidation phase are shown in Fig. 9.

Considering a quasi-saturated state also the time for the consolidation increases. Due to the increased compressibility it lasts longer to reduce excess pore water pressures. In contrast the consolidation is faster for stiffer soils.

4.4 Evaluation of the influence of permeability and quasi-saturation on soil behaviour with Mohr-Coulomb model

4.4.1 Introduction

To evaluate the influence of the permeability and the quasi-saturated state, calculations with the linear-elastic perfectly-plastic Mohr-Coulomb model are performed. For the calculations a fully saturated state is assumed on the one hand and on the other hand a partially saturated stated (including quasi-saturation) is considered. Therefore, again a value for the bulk modulus of the pore fluid of K_{wg} = 10 000 kN/m² is used. Furthermore, a soil water characteristic curve is used. Within this calculations the influence of the stiffness is neglected and only a Young's modulus *E'* which corresponds to oedometer stiffness E_{oed} = 15 000 kN/m² is used (E' = 10 120 kN/m²). Calculations are carried out using different values of permeability, a higher one, a lower one and two different permeabilities for the slope and the subsoil.

- k = 1E-7 m/s (corresponds to 0.00864 m/day)
- k = 1E-4 m/s (corresponds to 8.64 m/day)
- k_{slope} = 1E-3 m/s (corresponds to 86,4 m/d) and $k_{subsoil}$ = 1E-7 m/s

Calculations considering partially saturation/quasi-saturation, using a constant K_{wg}, are only performed in case of k = 1E-7 m/s, since the results from the linear-elastic analysis show no differences using a high permeability. The introduced soil water characteristic curve is used for k = 1E-7 m/s as well as k = 1E-4 m/s.

The pore water pressures in case of different *k* values are only evaluated in node D. Node D is located beneath the dam in the subsoil. The nodes A and B are the same like those from the linear-elastic calculations. A new node (node C) is introduced to evaluate the pore pressures at the inside of the dam at a higher location.

Using the Mohr-Coulomb model, not only the case of a rapid drawdown is analysed. A slow drawdown is also investigated to show the influence of the drawdown velocity.

For the calculations using a defined soil water characteristic curve, a curve following cubic law is used to describe the relative permeability. The soil water characteristic curve (SWCC) is implemented with Tab. 5.

$$k^{rel} = k^{sat} * S_r^3 \quad (17)$$

k^{rel}	[m/s]	Relative permeability
k_0	[m/s]	Permeability at the boundary to unsaturated zone
k^{sat}	[m/s]	Saturated permeability

Tab. 5 Soil water characteristic curve

Saturation S	Capillary height $-\psi$	Relative permeability k_{rel}
1,00E-04	100	1,00E-04
0,6757	10	0,3085
0,75289325	3	0,42677622
0,81708635	1	0,54551145
0,83466817	0,7	0,58148907
0,84913336	0,5	0,61224848
0,86678946	0,3	0,65123969
0,87719428	0,2	0,67497451
0,89005853	0,09	0,7051081
0,9	0	0,729
0,92519374	-3	0,79195053
0,93140154	-4	0,80799905
0,93684941	-5	0,82226038
0,94166885	-6	0,83501564
0,94596266	-7	0,84649028
0,94981238	-8	0,85686713
0,95642933	-10	0,87490049
0,96857512	-15	0,90865689
0,97684515	-20	0,93213148
1	-100	1

4.4.2 Results on study using Mohr-Coulomb model

Results depicted in the following figure (Fig. 10) represent the pore water pressure development in node A using the MC model for rapid drawdown. Like in the linear-elastic calculations the node is located at the right limit of the model 5 m beneath the surface. At this node 1D conditions can be assumed.

The results with a permeability of k = 1E-4 m/s (yellow line in Fig. 10) show that pore water pressures in node A change simultaneously with the water level. Even for the calculations with a soil water characteristic curve, including the quasi-saturated range (blue line in Fig. 10), approximately hydrostatic pore pressure conditions result. Calculations with a low permeability of k = 1E-7 m/s (represented by the black line) show a small amount of excess pore water pressure but this is a numerical issue.

Considering quasi-saturation (represented by the red, green and blue lines) it can be seen, that higher excess pore pressures are produced, due to the increased compressibility of the pore fluid. Using the soil water characteristic curve instead of a constant increased compressibility, even higher pore pressures develop. Considering, for node A, quasi-saturation, equation (4) can be applied because no deviatoric stress is applied. This results from the fact that for linear-elastic 1D compression the deviatoric component cancels out as the A coefficient gets 1/3.

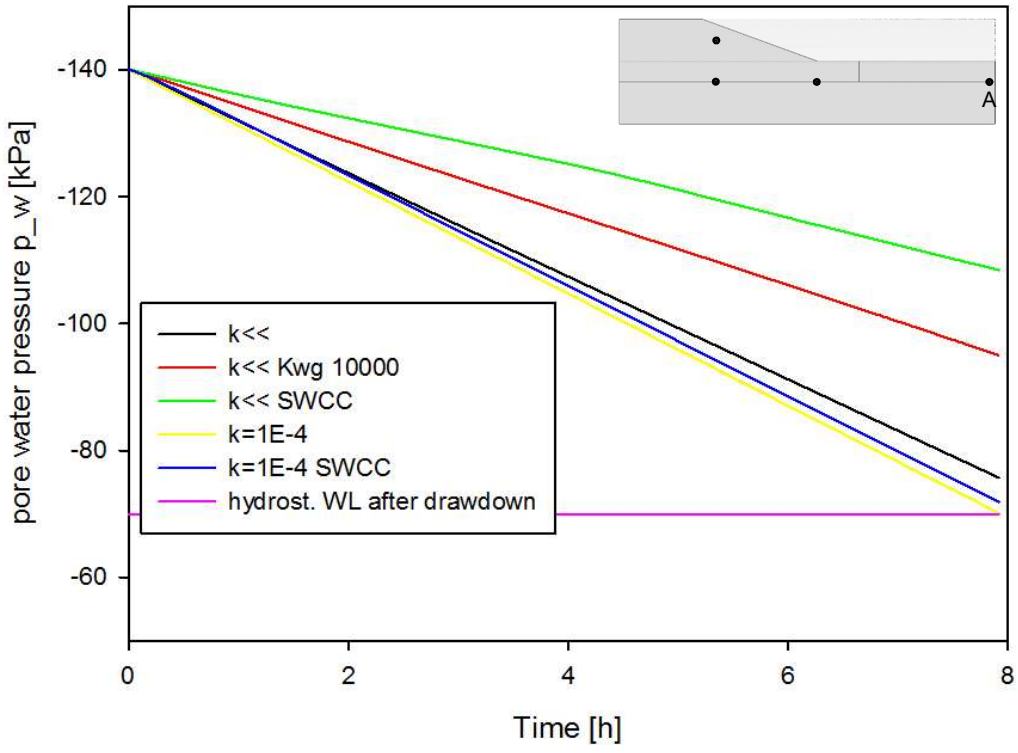

Fig. 10 Results for pore water pressure in node A – rapid drawdown

The pore water pressures after a slow drawdown event with a drawdown rate of 1 m/d (shown in Fig. 11) clearly differ from those of a rapid one. Considering a fully saturated soil (black and yellow lines in Fig. 11), all calculations show approximately hydrostatic conditions after the drawdown. Using a high permeability of k = 1E-4 m/s, either with a considered fully saturated state (yellow line) or the implemented soil water characteristic curve (blue line), lead nearly to the same results. The little amount of excess pore water pressure resulting from the calculation using a permeability of k = 1E-7 m/s is again due to the numerical procedure.

Using a constant pore fluid bulk modulus (represented by the red line) the results are not as high as with the soil water characteristic curve (green line), when a low permeability is considered (k = 1E-7 m/s). But due to the undrained behaviour and the introduced constant pore fluid bulk modulus K_{wg}, higher than considering a fully saturated state.

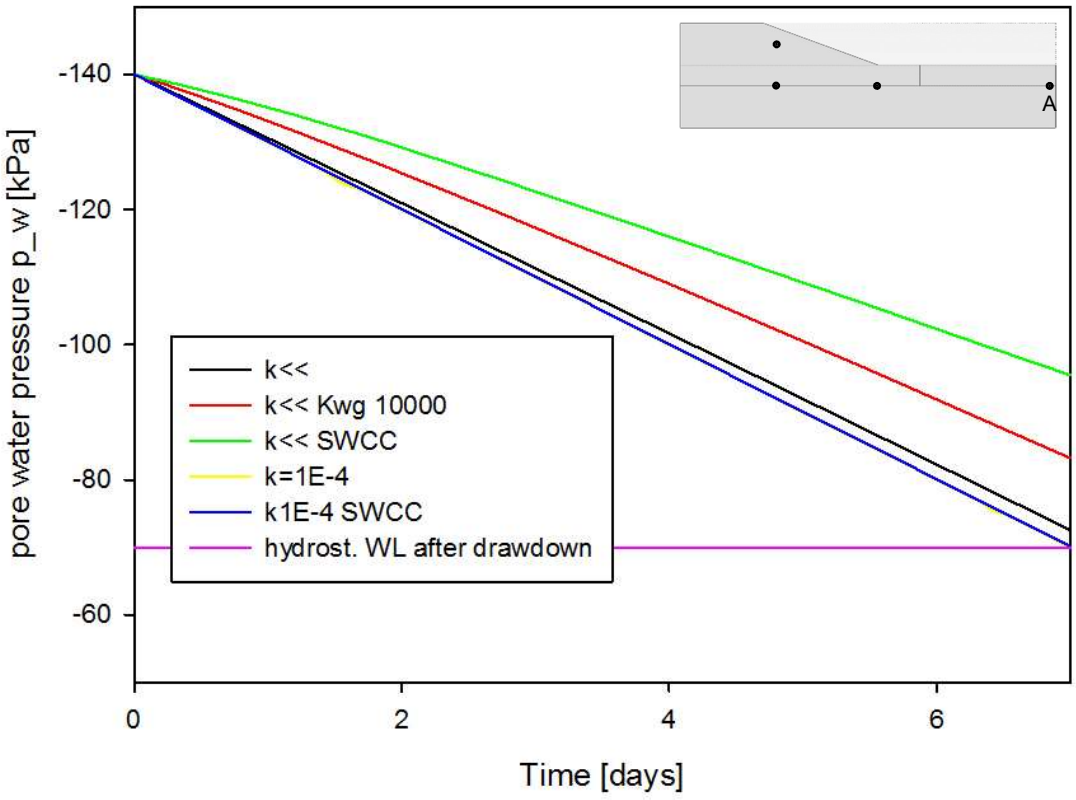

Fig. 11 Results for pore water pressure in node A – slow drawdown

Fig. 12 shows the results for pore water pressures in node B and D for rapid drawdown. As mentioned before, node D (see pink line in Fig. 12 and Fig. 13) is only used for evaluating the pore water pressures in case of two different permeabilities for the slope and subsoil.

Due to the location of node B, changes in deviatoric stresses are produced due to the water level change. The removed stabilizing water body on the slope surface will cause a downwards movement of the slope. This effect causes shear stresses and a slip surface may develop. Those shear stresses have also an effect on the pore pressure development in node B. For k = 1E-7 m/s and 1E-4 m/s considering full saturation this can be seen in Fig. 12 (see black and yellow line respectively). Again considering a quasi-saturated state leads to the highest excess pore water pressures for both used permeabilities (red, green and blue lines).

In case of nearly undrained conditions the excess pore pressures in node B can also be explained with the theory according to Skempton (1954). But due the influencing shear component the simplified equation (1) cannot be applied. In this case also the Skempton *A* parameter has to be considered. This parameter reflects the influence of a changing in deviatoric stresses ($\Delta\sigma_1$ - $\Delta\sigma_3$). Here the complete equation of Skempton has to be applied. (Skempton 1954).

$$\Delta p_{water} = B * [\Delta p * \frac{3A - 1}{3} * \Delta q] \quad (18)$$

Δp_{water}	[kN/m²]	change in pore water pressure
B	[-]	Skempton *B* parameter
A	[-]	Skempton *A* parameter
Δp	[kN/m²]	Change in total mean stress
Δq	[m]	Change in deviatoric stress

High permeabilities lead to hydrostatic pressure conditions after the drawdown which is again caused by the drained behaviour of the soil.

In case of two different permeabilities for the slope and the subsoil, the water level in the slope changes simultaneously with the external water level. This leads to a change of the soil unit weight (γ' gets to γ_{unsat}) and furthermore to a change in total stresses at the top of the low permeable subsoil. Due to the change in total stress, excess pore pressures are produced in node D according to Skempton's theory (1954).

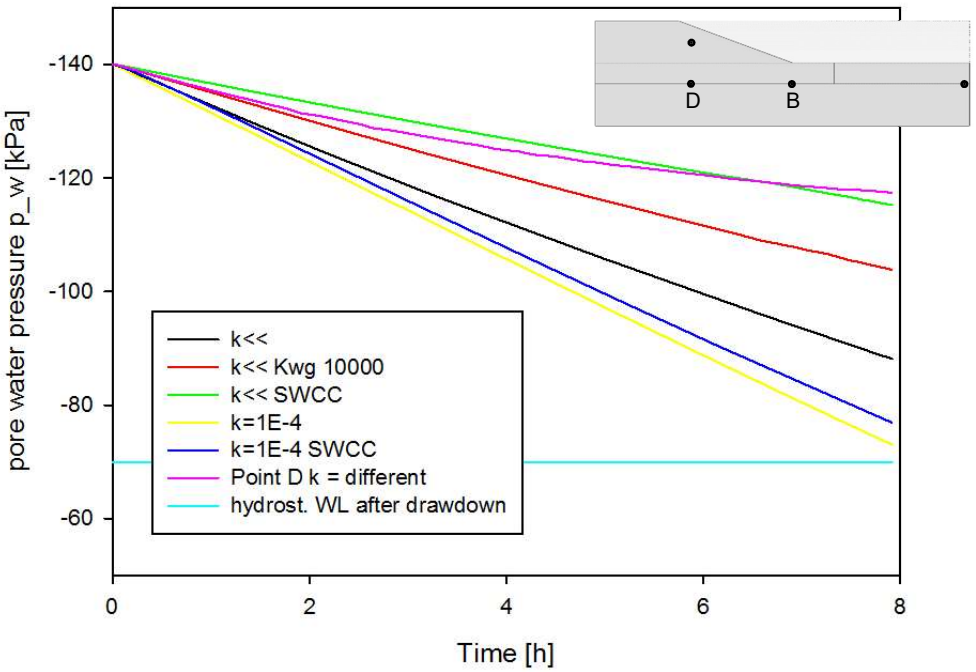

Fig. 12 Results for pore water pressure in node B (D) – rapid drawdown

As well as in node A for slow drawdown also in node B the excess pore pressures are smaller after a slow drawdown (see Fig. 13). This results from the fact that due to the slow lowering of the water, the excess pore pressures have more time to dissipate, even with low permeabilities. Although they are significantly higher in node B than in node A as the shear component has also an influence on the excess pore pressure. In contrast to the rapid drawdown also the result for node D show smaller excess pore water pressures.

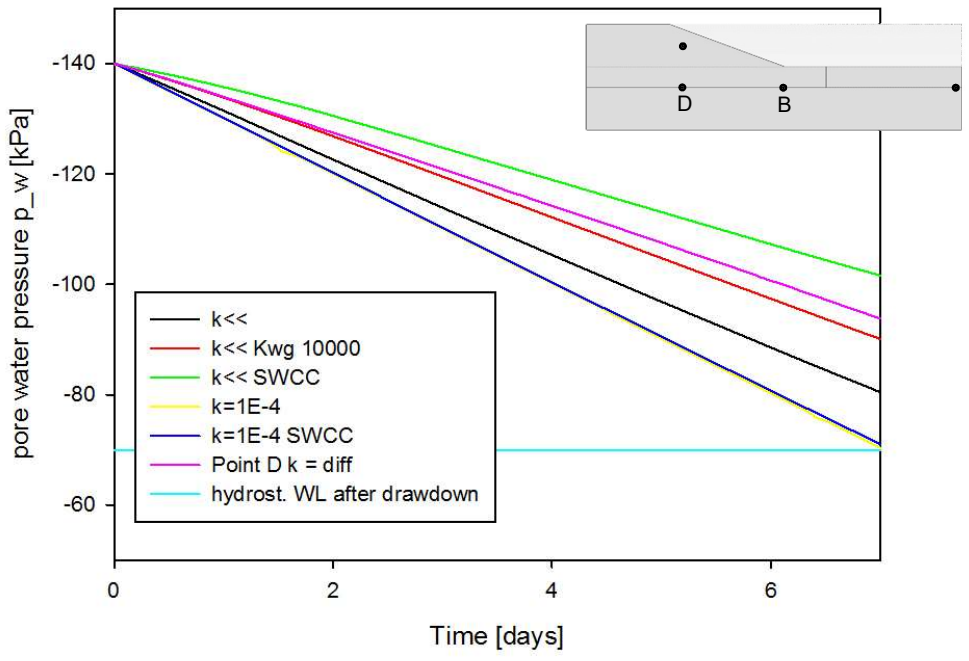

Fig. 13 Results for pore water pressure in node B (D) – slow drawdown

In node C, pore pressures decrease simultaneously with the water level in case of a high permeability. Once the water level has lowered below node C the effect of suction occurs.

In contrast, simulations with low permeability show that the internal water level remains higher and so does the pore water pressure, even for the used soil water characteristic curve. The slight increase in pore water pressure at the end for low permeability arise from the deformations which occur during the drawdown.

The difference in the pore water pressure development between the rapid drawdown and the slow drawdown (cmp. Fig. 14 and Fig. 15) results mainly from the different ground water levels in the slope after the water level lowering.

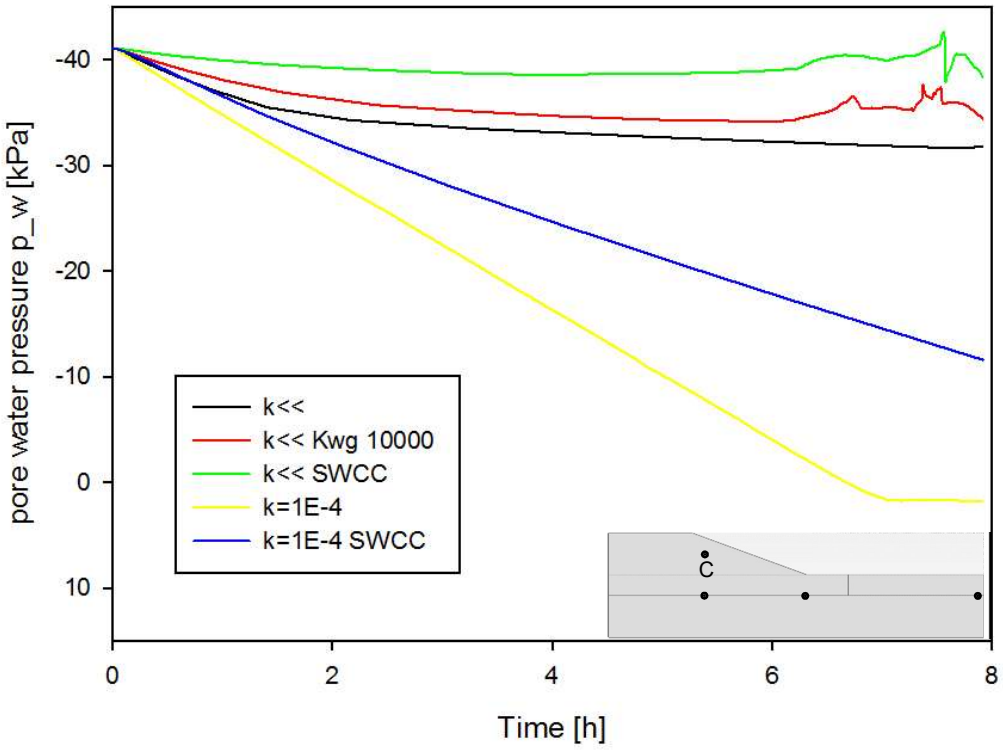

Fig. 14 Results for pore water pressure in node C – rapid drawdown

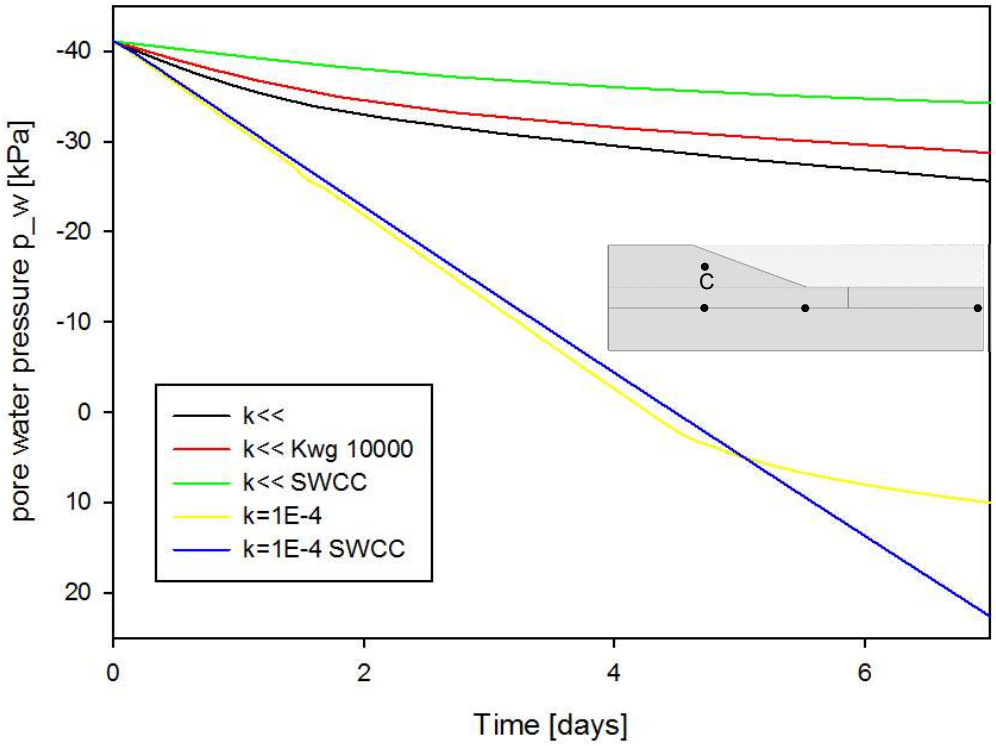

Fig. 15 Results for pore water pressure in node C – slow drawdown

Observing the results of the performed consolidation (see Fig. 16 and Fig. 17) a clear difference between the calculations for the different permeabilities can be seen. Considering a high permeability the hydrostatic water pressure is reached directly after the drawdown independently of the drawdown rate. Due to the lower pore pressures after slow drawdown the consolidation starts slower.

Pore pressures remain higher after 100 days using a constant K_{wg}, due to the increased compressibility of the pore fluid and the fact that no stress dependent stiffness is considered in the Mohr-Coulomb model. As the compressibility has no constant value in SWCC pore pressures are lower after 100 days.

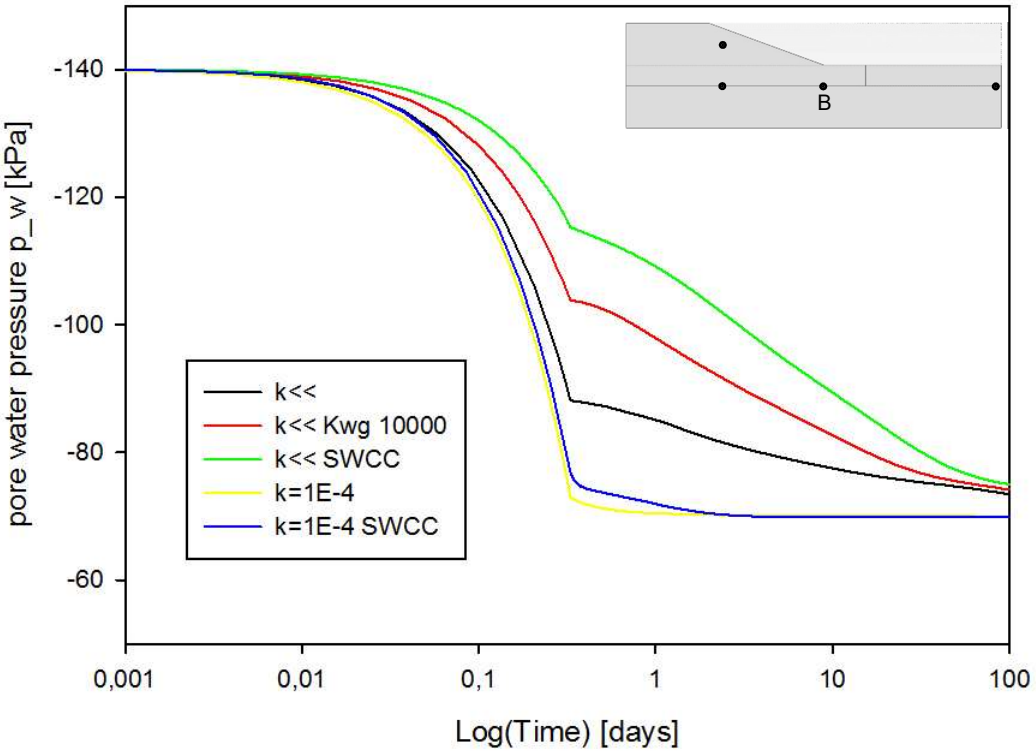

Fig. 16 Results for consolidation in node B – rapid drawdown

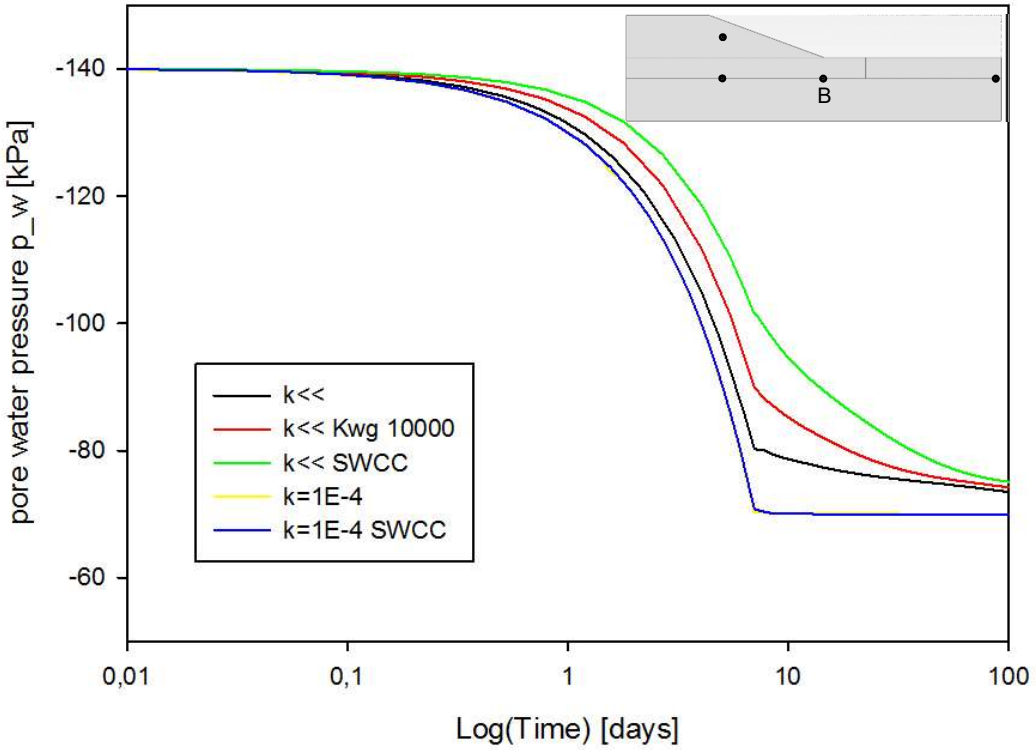

Fig. 17 Results for consolidation in node B – slow drawdown

4.5 Calculations using the Hardening Soil Small model

4.5.1 Introduction

Calculations using the Hardening Soil model with small strain stiffness are carried out considering a fully saturated state on the one hand and a quasi-saturated state on the other hand. In this case only a permeability of k = 1E-7 m/s is considered. The quasi-saturation is considered again by applying a constant pore fluid bulk modulus of K_{wg} = 10 000 kN/m² instead of a soil water characteristic curve. The performed calculations are compared with those of the linear-elastic study. Material parameters can be seen in Tab. 4.

At the beginning, the drawdown scenario was performed with a linear-elastic model, using different stiffnesses. The applied stiffness parameters correspond to the primary loading, un-/reloading and small strain stiffness. In the following the results of the linear-elastic model are compared with results from a drawdown analysis with the HSS model. This comparison should show, which stiffness controls the soil behaviour during a drawdown scenario if the HSS model is applied. Previous analysis showed that a slow drawdown rate causes no high excess pore water pressures. Therefore only a rapid drawdown is analysed with the HSS model.

4.5.2 Results of calculations with Hardening Soil Small model

As well as for the other constitutive models, the calculations with the HSS model show a nearly simultaneously change of pore water pressures with decreasing water level in node A when a fully saturated soil is considered. Using a decreased pore fluid bulk modulus K_{wg}, excess pore water pressures occur even in node A. Due to the low value for B, just a small amount of the load change is transferred to the water, the complement of (B-1) of the load which is transferred to the soil skeleton produces excess pore water pressures.

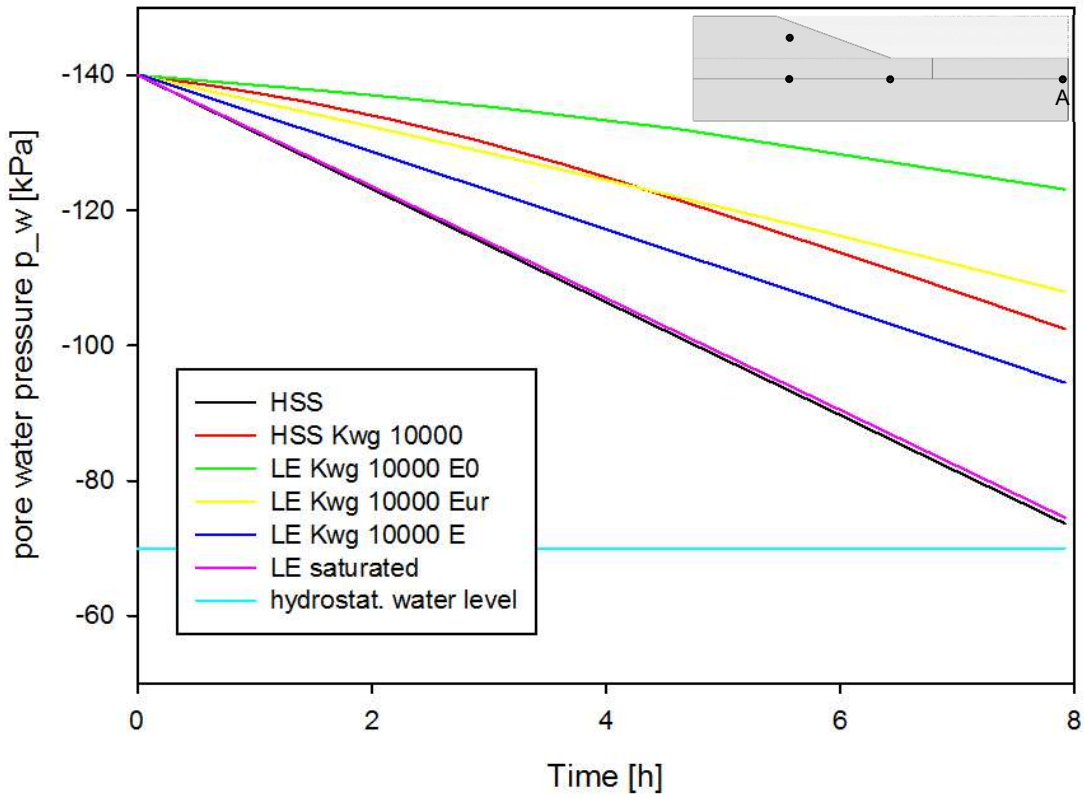

Fig. 18 Results for pore water pressure in node A – rapid drawdown with HSS model

The comparison with the linear-elastic calculations show that the pore pressures considering a fully saturated soil as well as a low permeability (k = 1E-7 m/s) are identically in node A for both constitutive models (black and pink lines). For the saturated linear-elastic calculation (pink line) a stiffness of E = 37 500 kN/m² is used (corresponds to the un-/reloading stiffness).

When a quasi-saturated state is considered, it can be seen that the results of the HSS model are comparable to the results of the linear-elastic model using un-/reloading stiffness (red and yellow lines). This shows that the behaviour during a drawdown is controlled by the un-/reloading stiffness. However, it has to be mentioned that prior to the drawdown an excavation phase was performed to calculate the initial stresses. This leads to a stress path inside the current yield surface and therefore the application of the un-/reloading stiffness is logical. The difference between the two results is due the stress dependent stiffness of the soil in the HSS model.

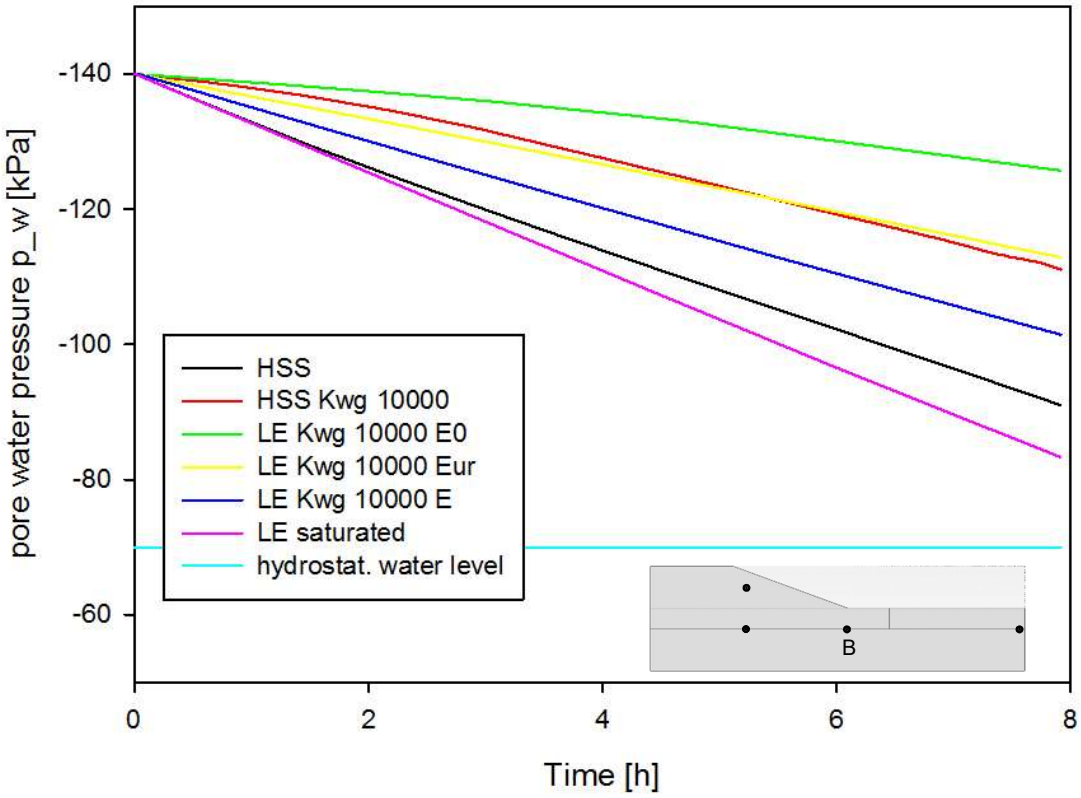

Fig. 19 Results for pore water pressure in node B – rapid drawdown with HSS model

According to Fig. 19 the calculation results for node B show different pore pressures for the linear-elastic and for the HSS model when the soil is considered as fully saturated (black and pink lines). The difference between the two models is due to the fact that the HSS model uses a stress dependent stiffness, whereas the linear-elastic model uses a constant stiffness value (E = 37 500 kN/m², this corresponds to the un-/reloading stiffness). As discussed already before, the magnitude of the excess pore water pressure depends strongly on the material stiffness.

Considering quasi-saturation the results show that the HSS model corresponds again to the linear-elastic model with un-/reloading stiffness.

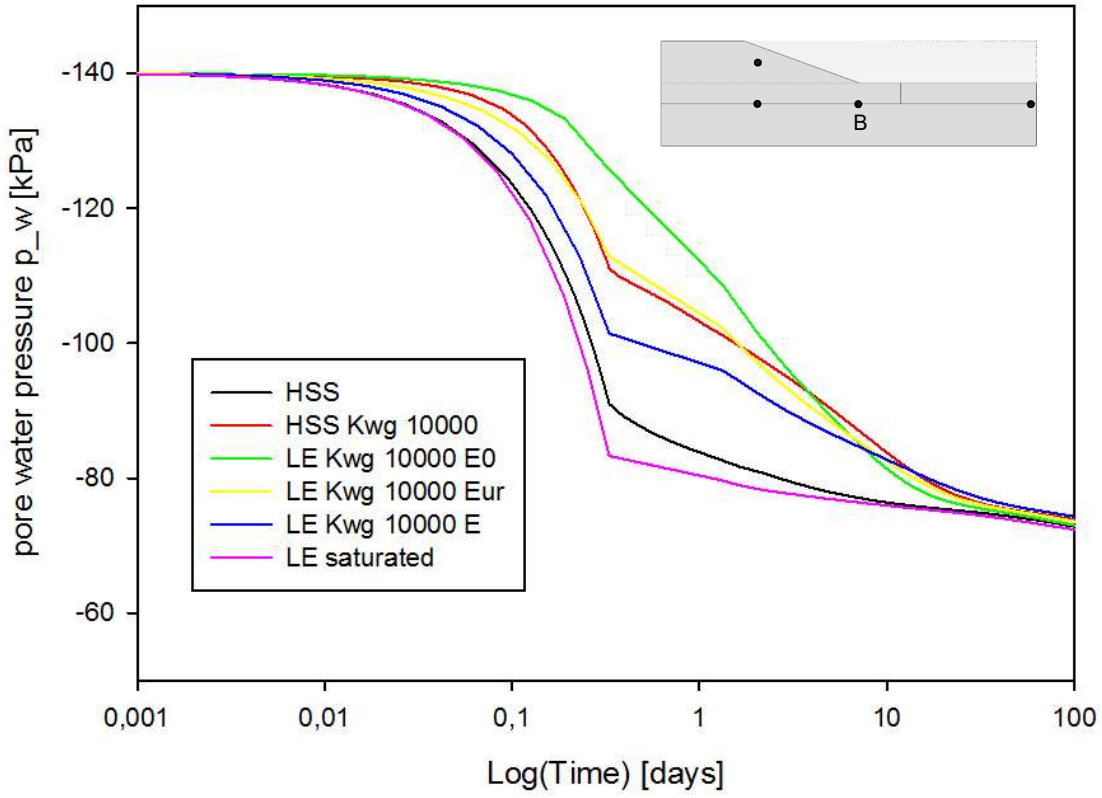

Fig. 20 Results for consolidation in node B – after rapid drawdown with HSS model

The evaluation of the performed consolidation also shows that fully saturated conditions lead to similar results for the linear-elastic and the HSS calculations. For the quasi-saturated case, the linear-elastic model with un-/reloading stiffness gives the best fit with the HSS model.

4.6 Conclusion

The main purpose of this study is to show the influence of entrapped air on the excess pore water pressure development during a rapid drawdown. The obtained results show a clear difference between a saturated and a quasi-saturated state. Considering a fully saturated soil, the developing excess pore water pressures are significantly lower than in a quasi-saturated state. It can be seen that even a small amount of entrapped air in the soil increases the compressibility of the pore fluid. This leads to a load distribution between soil skeleton and pore fluid. The ratio between the bulk modulus of the soil skeleton and the bulk modulus of the pore fluid has an influence on the excess pore water pressure development.

In the course of this study the influence of the soil permeability and the drawdown velocity on the pore water pressure development were investigated. It shows that for slow drawdown rates (even for lower permeable soils) as well as for high permeable soils

(also in case of a rapid drawdown) the development of excess pore water pressures can be neglected.

Whereas a low permeable soil combined with a high drawdown velocity leads to high excess pore water pressure even for saturated conditions in the range of the slope toe (cmp. node B). However considering a quasi-saturated state developing excess pore pressures are in fact significantly higher.

In summary it can be said that for a reliable prediction of the resulting pore water pressures due to a drawdown scenario, a correct estimation of the degree of saturation (amount of entrapped air), the soil stiffness and the soil permeability is necessary.

5 Influence of degree of saturation on the soil behaviour during water level changes

5.1 Introduction

The experiences from the preliminary study are applied now to investigate the influence of partially saturation and quasi-saturation on the pore water pressure development and the slope stability of a real project. Therefore, an already finished flood protection dam, located in Upper Austria is analysed, considering different degrees of saturation.

To determine the missing strength parameters, the results of the first calculations are compared to already existing limit equilibrium analyses. Then calculations, ignoring the influence of suction, are performed for two load cases. Afterwards, the influence of partially saturation is then investigated by applying soil water characteristic curves to the submerged materials. In a first step, soil water characteristic curves, which are available in Plaxis2D 2016 are used. In a second step, a user-defined SWCC, including the quasi-saturated range is applied to estimate the influence of quasi-saturation on the soil behaviour and the safety factor of the slope.

5.2 Project description

The project, located in Upper Austria, is a retention basin with a capacity of approximately 756 000 m³ and serves as a flood protection.

The dam has an upstream inclination of 1:2.2 and a downstream inclination of 1:4. The central core of the dam is constructed with loess clay (alluvial sediments) and covered with a 0.7 m thick layer of angular gravel. To support the core, a supporting body is constructed on the downstream side by using round gravel. On the downstream side a filter body is constructed as well.

The subsoil in this region consists mainly of sandy, silty clay with small sand layers. These layers are based on tertiary sediments which are referred to as marl.

5.3 Model for the representative cross section

At the beginning the design cross section was modelled in a CAD program and then implemented in Plaxis2D 2016. Dimensions of the dam were assumed according to the technical report of the project.

The model consists of a sandy gravel layer located on the marl (deepest layer). A silt layer is located on the sandy gravel layer. A part of the silt layer, in the area of the dam, was excavated in order to construct the dam. The dam exists of the core, the support body and the top gravel (core cover). The sandy gravel layer is approximately 1.6 m thick and the silt layer on top is approximately 1 m. At the upstream side the dam height from the river bed to dam crest is 9.7 m.

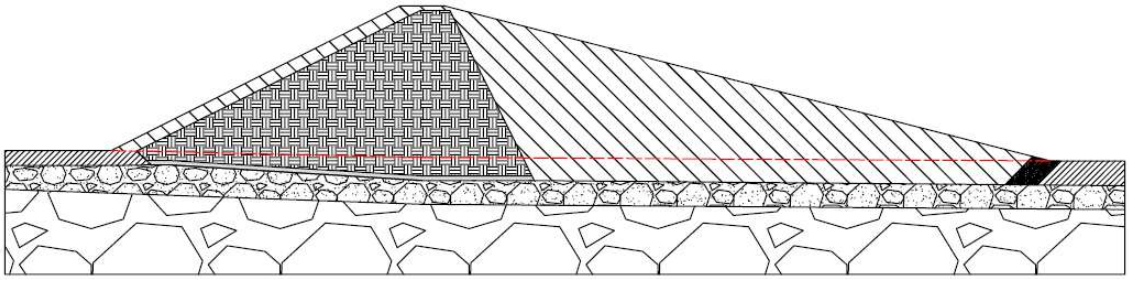

Fig. 21 CAD model of the design cross section

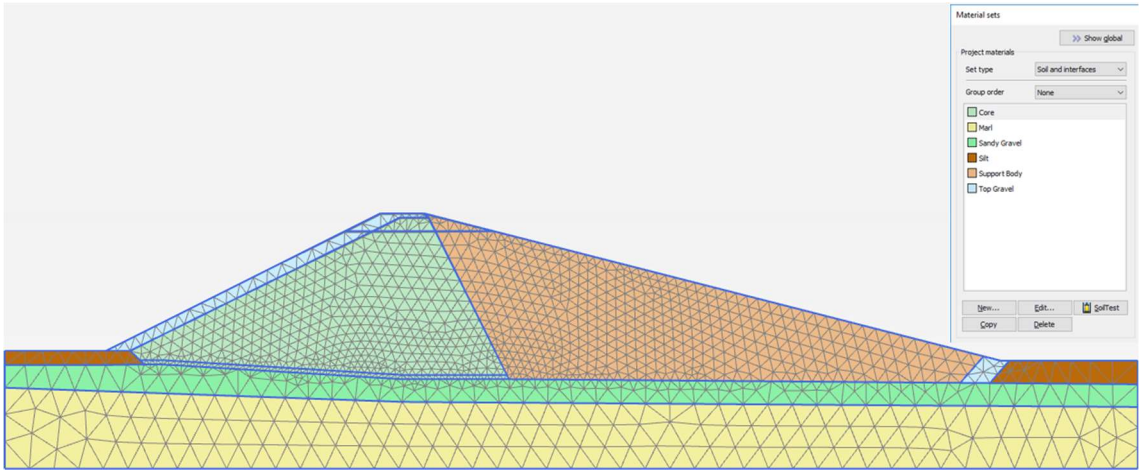

Fig. 22 FE – model of the design cross section with material allegation

The model is generated with 2,482 15-noded elements and 20,173 nodes. Corse grained soils are modelled with the Mohr-Coulomb constitutive model and fine grained soils are modelled with the Hardening Soil model with small strain stiffness (HSS model). A list with the material definition is shown in Fig. 22.

5.4 Parameter determination

5.4.1 General Parameters

Due to the fact that not all parameters were given in the technical report, some had to be assumed. Concerning the strength parameters, only the friction angle of the core and of the supporting body were known. Furthermore, the permeability of the core and the silt layer were mentioned in the report. Tab. 6 and Tab. 7 show the used parameters.

Permeabilities of the different soils are estimated on the basis of the known grain size distribution. The procedure according to Hazen (1893) for the permeability estimation is only valid for a degree of irregularity of U < 5. According to Beyer (1964) the permeability can be also estimated on the basis of the grain size distribution for degrees of irregularity of U > 5. Therefore Beyer (1964) introduced a factor of correction *c(U)*. Beyer provides different factors of correction for the range of 1 < U < 20 and for U > 20 (c(U) = 0.006 for U > 20) (Odenwald et al 2009). Due to the irregularity of the grain size distribution of the present soils on site the approach according to Beyer is used. The support body and the sandy gravel have a degree of irregularity of U = 53 and U = 58 respectively.

$$U = \frac{d_{60}}{d_{10}} \; and \; k = c(U) * d_{10}^2 \qquad (19)$$

U	[-]	Degree of irregularity
d_{60}, d_{10}	[mm]	60% or 10% sieve pass through respectively
k	[m/s]	Permeability
c(U)	[]	Factor of correction (0.006 for U > 20)

The sandy gravel layer and the support body of the dam show a characteristic grain size of d_{10} = 0.13 and 0.20, respectively (according to the grain size distribution in the technical report). This results in a permeability of k = 1.04E-4 m/s for the sandy gravel layer and k = 2.4E-4 m/s for the support body. The permeability of the top gravel is assumed to be equal to the supporting body as it is the same material (but angular). For the marl layer a permeability of 1E-7 m/s is assumed.

Except for the friction angle of the core and the support body all other strength parameters are assumed. The friction angle for the top gravel is assumed to be slightly higher than of the support body as it is angular.

Other strength parameters were back calculated. For this purpose comparative calculations of a FE safety analysis and limit equilibrium analysis from the technical report were conducted. Two different load cases are investigated. A filled reservoir after a flood event (HQ100) and a drawdown event with a drawdown rate of 6.83 m/18 h (corresponds to 0.38 m/h). Both cases are analysed with a non-associated flow rule as well as with an associated flow rule. The strength parameters have been adjusted to get the best fit between the results of the FEA and the limit equilibrium analysis for the failure mechanism and the factor of safety. The back calculated strength parameters lead to factors of safety which differ approximately ± 10% from the results of the technical report,

depending on the used flow rule and load case. Typical failure mechanisms are shown in Fig. 23 for a non-associated calculation.

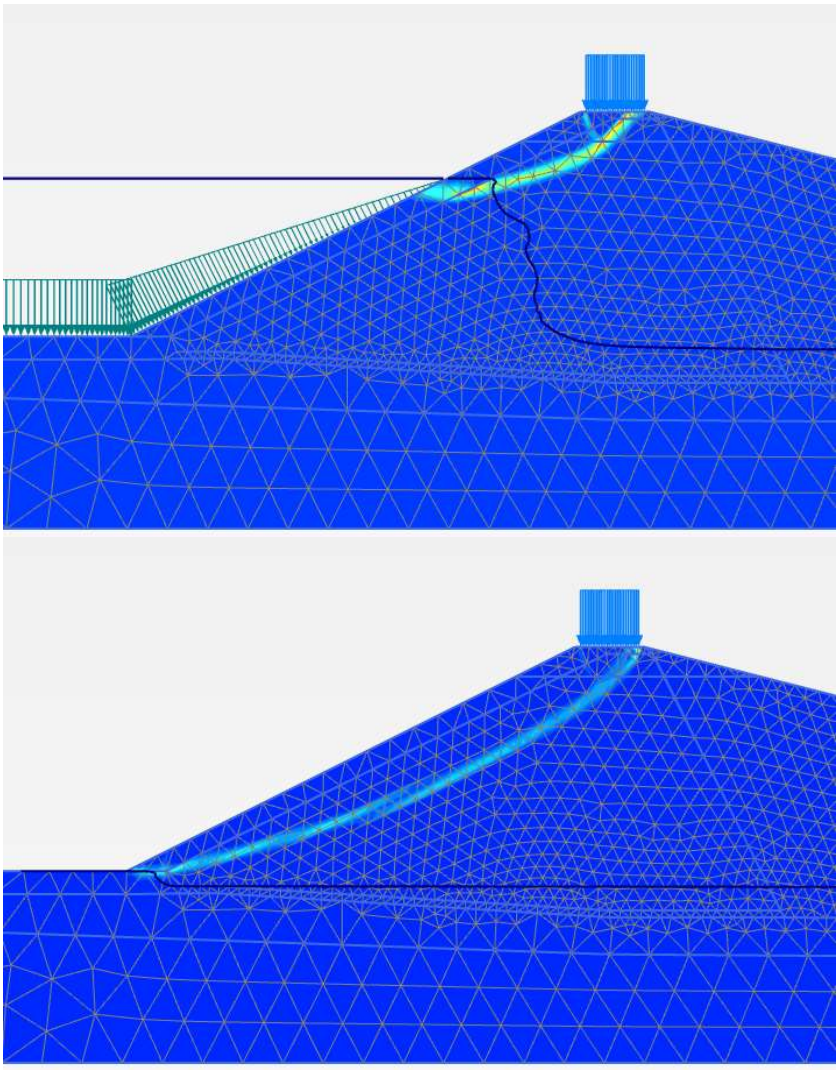

a.)

b.)

Fig. 23 Failure mechanisms displayed with deviatoric strains for a.) Filled reservoir and b.) After rapid drawdown

For the support body and the core, plate-loading tests were performed. The obtained deformation modulus E_v is used to determine the Young's modulus (after Goodman 1980) which is used in a next step to determine E_{oed}.

$$E' = E_v * (1 - \nu^2) \quad (20)$$

E'	[kN/m²]	Young's modulus
E_v	[kN/m²]	Deformation modulus of plate-loading test
ν	[-]	Poisson's ratio

$$E_{oed} = \frac{(1-\nu) * E}{(1-2\nu) * (1+\nu)} \quad (21)$$

E_{oed} [kN/m²] Oedometer modulus

This leads to a Young's modulus for the support body of E´ = 54 400 kN/m² and to an oedometer modulus for the core of E_{oed} = 27 500 kN/m² when a Poisson's ratio of ν = 0.33 is assumed. Additional stiffness parameters for the HSS model are estimated on basis of the oedometer modulus.

Tab. 6 Parameters for soils with Mohr-Coulomb model

		Sandy Gravel	Marl	Support Body	Top Gravel	
Parameter		**Value**				**Unit**
Material model		MC	MC	MC	MC	[-]
Saturated unit weight	γ_{sat}	21.5	26	21	21	[kN/m³]
Dry unit weight	γ_{unsat}	19	26	19	19	[kN/m³]
Drainage type		Drained	Undrained	Drained	Drained	[-]
Young's modulus	E´	35 000	80 000	54 400	54 400	[kN/m²]
Poisson's ratio	ν	0.33	0.33	0.33	0.33	[-]
Cohesion	c	1	0	0	1	[kN/m²]
Friction angle	φ	34	36	38.5	43	[°]
Dilatancy angle	ψ	0	0	0	0	[°]
Permeabilities	$k_{x,y}$	1.04E-4	1E-7	2.4E-4	2.4E-4	[m/s]

Tab. 7 Parameters for soils with Hardening Soil Small model

		Silt	Core	
Parameter		**Value**		**Unit**
Material model		HSS	HSS	[-]
Saturated unit weight	γ_{sat}	19	20	[kN/m³]
Dry unit weight	γ_{unsat}	18	19	[kN/m³]
Drainage type		Undrained	Undrained	[-]
Triaxial stiffness	E_{50}	22 000	36 500	[kN/m²]
Oedometer stiffness	E_{oed}	18 000	27 500	[-]
Un-/reloading stiffness	E_{ur}	48 400	73 000	[kN/m²]
Power of stress dependency	m	0.7	0.7	[-]
Cohesion	c	2.5	3.5	[kN/m²]
Friction angle	φ	27	27.5	[°]
Dilatancy angle	ψ	0	0	[°]
Small strain shear modulus	G_0	80 650	109 000	[kN/m²]
Shear strains at 70% of G_0	$\gamma_{0.7}$	0.0001	0.0001	[-]
Poisson's ratio for un-/reloading	ν_{ur}	0.2	0.2	[-]
Permeabilities	$k_{x,y}$	3.1E-8	1.18E-9	[m/s]

5.4.2 Parameters for partial saturation

For the later performed partially saturated analyses it is necessary to consider a soil water characteristic curve. Therefore, such curves are applied to the materials for the top gravel and the core as well as for the silt and the sandy gravel. The used curves are based on the Van Genuchten model with parameters from the Hypres (Hydraulic Properties of European Soils) database. For the top gravel a predefined curve of a coarse topsoil is used and for the core a predefined curve of a fine subsoil is used. Furthermore, for the silt and the sandy gravel the curves of a medium fine subsoil and a coarse subsoil are used.

The Van Genuchten model (based on Van Genuchten 1980) is one of the most common models to describe the relationship between suction and degree of saturation of partially saturated soils. (Galavi 2010)

$$S(\phi) = S_{res} + (S_{sat} - S_{res}) * [1 + (g_a + |\phi|)^{g_n}]^{g_c} \quad (22)$$

$S(\phi)$	[-]	Suction head depending on degree of saturation
S_{sat}	[-]	Saturated degree of saturation
S_{res}	[-]	Residual degree of saturation
ϕ	[m]	Suction head (defined by $-p_w/\gamma_w$)
g_a	[1/m]	Fitting parameter related to the air entry value of the soil
g_n	[-]	Fitting parameter of the rate of water extraction when the air entry value is exceeded
g_c	[-]	Fitting parameter to make a two parameter equation

The fitting parameter g_c is used to convert the Van Genuchten equation (25) into a two parameter equation. Therefore the following assumption is made in Plaxis2D 2016 (Brinkgreve 2016).

$$g_c = \frac{1 - g_n}{g_n} \quad (23)$$

Usually, the fitting parameters are determined with laboratory tests. In the current case they are taken from the Hypres database. The parameters of the used curves are shown in Tab. 8.

Tab. 8 Hydraulic properties of soil (Brinkgreve 2016)

		Topsoil Coarse	Subsoil Fine	Subsoil Medium Fine	Subsoil Coarse	Unit
Saturated water content	θ_s	0.403	0.481	0.412	0.366	[-]
Saturated saturation	S_{sat}	1.0	1.0	1.0	1.0	[-]
Residual water content	θ_r	0.025	0.010	0.010	0.025	[-]
Residual Degree of saturation	S_{res}	0.062	0.0208	0.0243	0.0683	[-]
Air entry parameter	g_a	3.83	1.98	0.82	4.3	[1/m]
Water extraction parameter	g_n	1.3774	1.0861	1.2179	1.5206	[-]

The applied soil water characteristic curves are shown in Fig. 24.

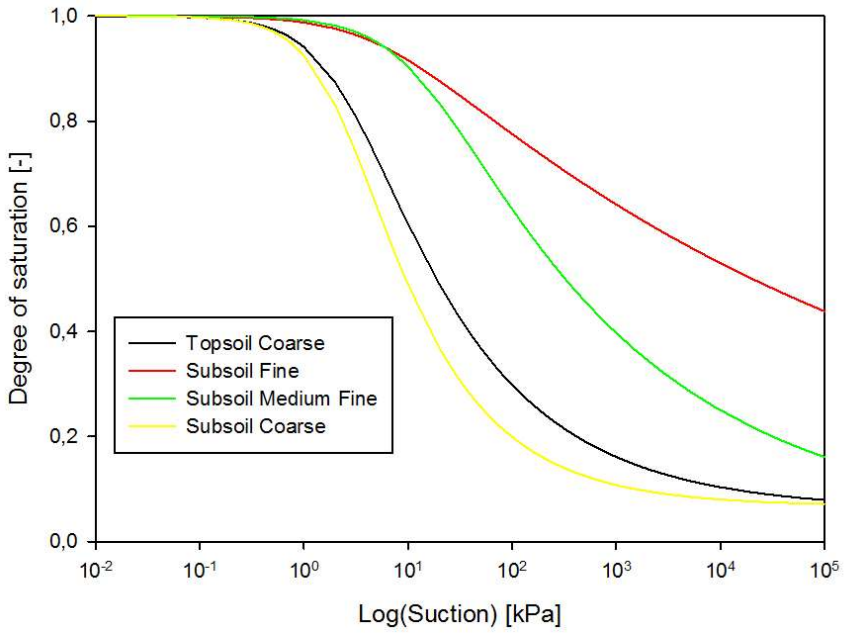

Fig. 24 Soil water characteristic curves based on the Van Genuchten equation

5.4.3 Parameters for quasi-saturation

For the analyses considering a quasi-saturated state (caused by entrapped air) below the phreatic level, the soil water characteristic curves of the fine grained materials are extended in the quasi-saturated range. For a degree of saturation S < 97% the standard soil water characteristic curves, based on the Hypres database are used. For a higher degree of saturation, the SWCC was defined according to equation (8) for the quasi-saturated state. The user-defined curves for the core material and the silt layer are displayed in Fig. 25.

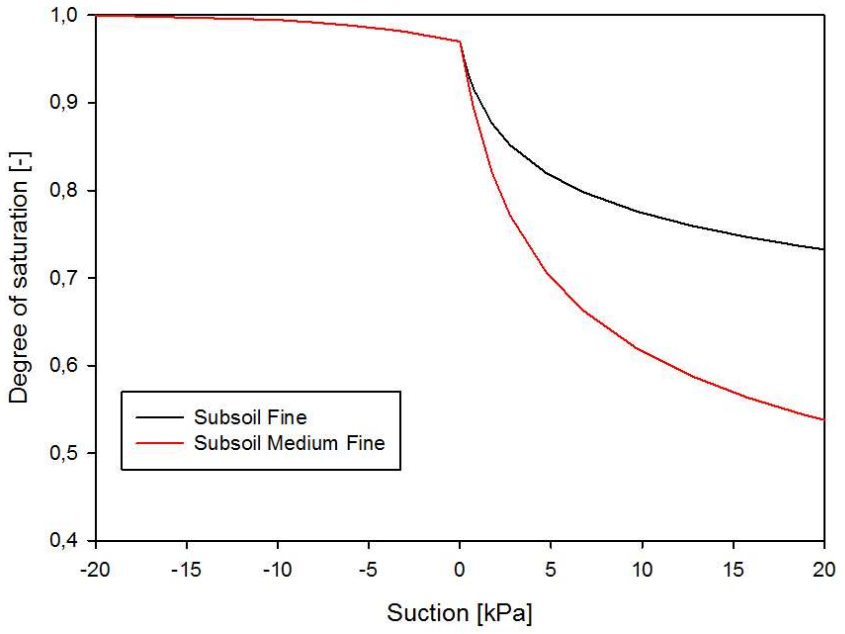

Fig. 25 Soil water characteristic curves

5.5 Investigated load cases and numerical setup

The numerical analyses are performed for several load cases and different states of saturation. Two steady state load cases are considered. A filled reservoir with an external water level of 6.83 m (water level after HQ100) and an empty reservoir with a water level at the ground surface. Furthermore, a fictitious rapid drawdown, where a steady state water level after HQ100 is lowered to the ground surface within 18h as well as the flood event HQ100 itself are simulated. During this flood event an impoundment and a subsequent drawdown take place.

The numerical analyses are performed with the following phases. In the initial phase a gravity loading is performed together with a steady state pore pressure calculation in order to get the correct water level in the dam. Phreatic levels are defined in the initial phase depending on the investigated load case. The initial phase is followed by a safety analysis. For the rapid drawdown and the HQ100 load case, two different hydraulic head functions are defined to simulate the water level change (change during the rapid drawdown is shown in Fig. 26). The water level changes are modelled with a fully coupled flow deformation analysis. During the rapid drawdown the water level is lowered 6.83 m in 18 h (corresponds to 0.75 days). The impoundment for the HQ100 of 6.83 m takes 10 h and is followed by a drawdown of 6.83 m in 15 h (related to the hydrograph for HQ100 shown in Fig. 26). Each of the mentioned load cases is followed by a safety analysis to evaluate the slope stability after the rapid drawdown, the impoundment of the HQ100 and the drawdown of the HQ100.

All the performed safety analyses consider an undrained material behaviour. Safety analyses with ignored undrained behaviour (drained) were also performed for all load cases and saturation states. In most cases the factors of safety and developing failure mechanisms are similar. However, in some cases the option ignore undrained behaviour led to not explainable failure mechanisms. Therefore, the undrained safety analyses were used to compare the factors of safety.

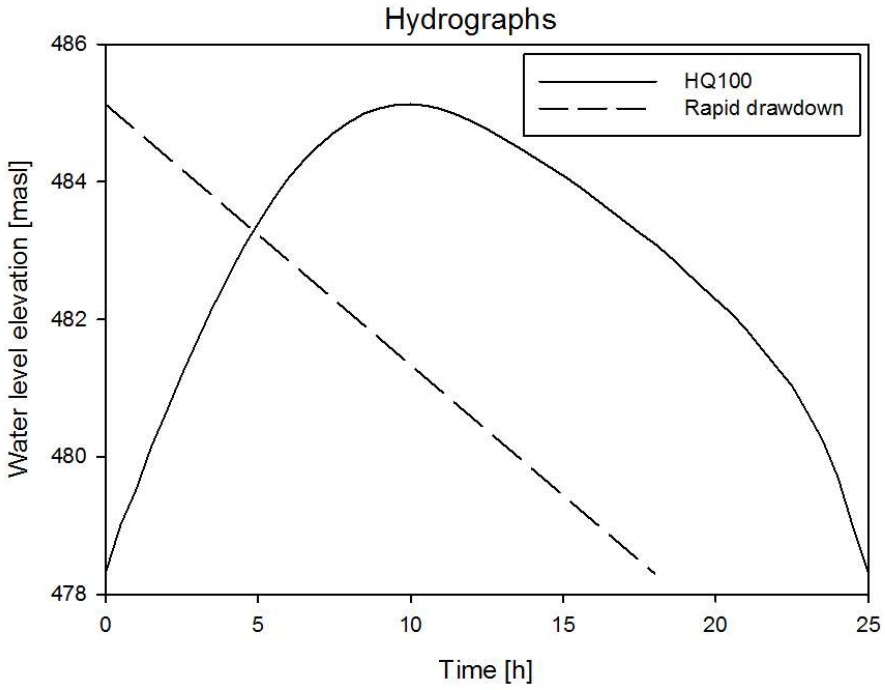

Fig. 26 Hydrograph for HQ100 and for the rapid drawdown

To investigate the pore water pressure development during the water level changes, four nodes inside the dam were selected for the following analysis. The selected nodes are shown in Fig. 27.

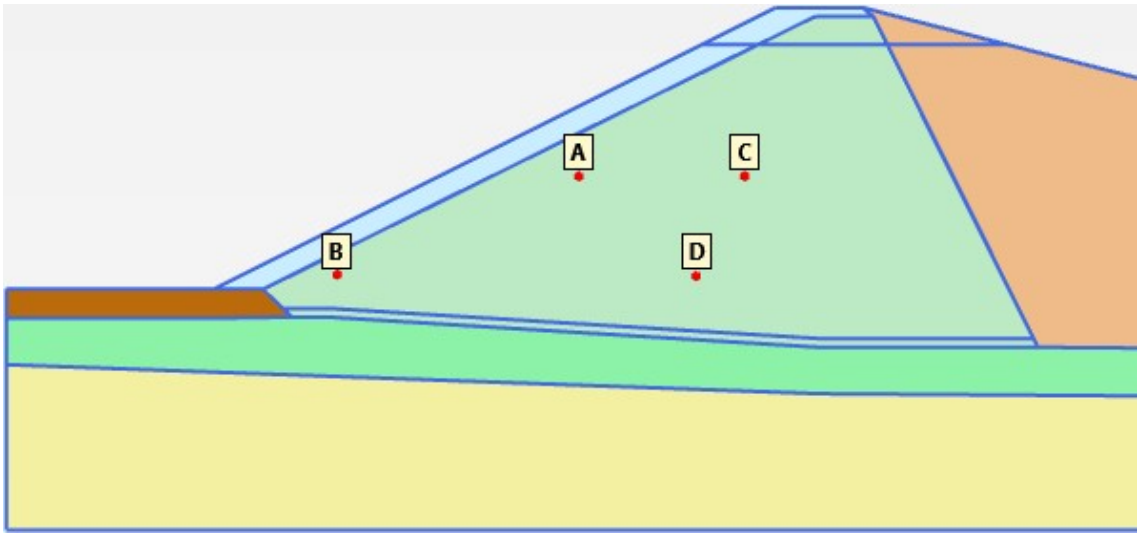

Fig. 27 Selected nodes for the calculations

5.6 Analyses without suction effects

To evaluate the soil behaviour following the principle of classical soil mechanics, where the soil behaves conventional above the phreatic level, two load cases are analysed. The load case of a filled reservoir and the load case of a rapid drawdown. A conventional soil (completely “dry”) above the ground water level means that the effects of suction are ignored.

5.6.1 Filled reservoir

The steady state water level for a filled reservoir is shown in Fig. 28. The developing failure mechanism is located in the area of the external water level as the lower part of the dam gets stabilized by the water.

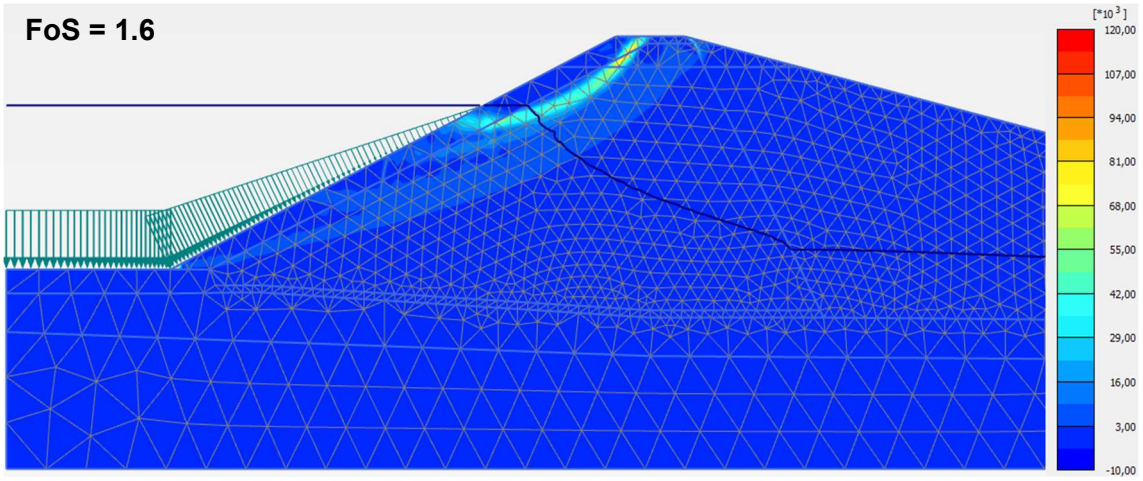

Fig. 28 Phase deviatoric strains for filled reservoir without suction after safety analysis

In this case the factor of safety is calculated as 1.6. As shown later, the factor of safety considering a partially or quasi-saturated state is higher, caused by the considered suction.

5.6.2 Rapid drawdown

A rapid drawdown in terms of classical soil mechanics leads to a failure of the dam. This results from the ignored suction which usually increases the effective stresses above the phreatic level inside the core.

The next figure (Fig. 29) shows the developing failure mechanism which results from the drawdown event.

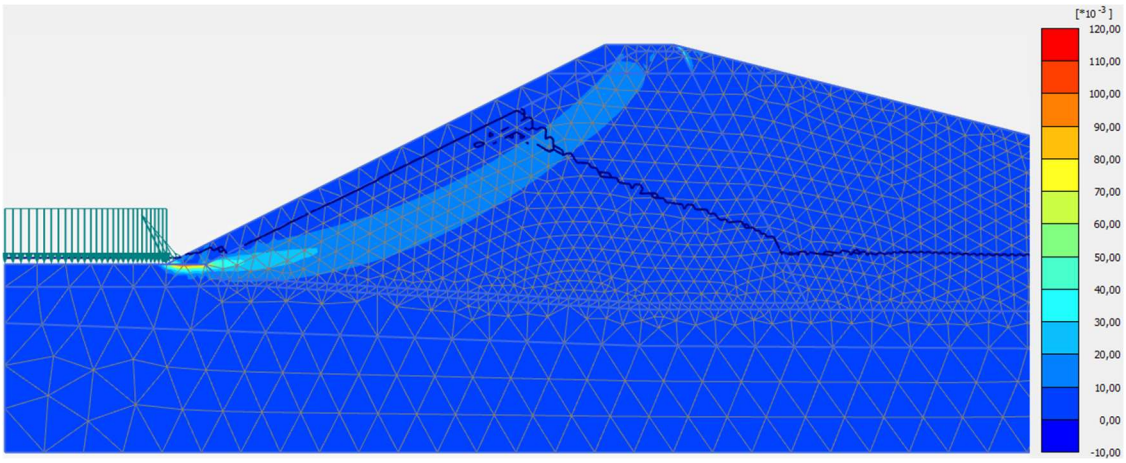

Fig. 29 Phase deviatoric strains after rapid drawdown without suction due to fully coupled flow deformation analysis

The figure above also shows that the failure happens almost at the end of the drawdown (M_{stage} = 0.959).

5.7 Partially saturated analysis

In order to investigate the influence of a partially saturated state on the pore water pressure development as well as the slope stability, the previous described project is analysed by applying the soil water characteristic curves to the materials according to chapter 5.4.2 (see Fig. 24).

5.7.1 Filled reservoir

For a filled reservoir the pore water pressures due to a steady state flow analysis as well as the factor of safety are determined. The steady state groundwater level is shown in Fig. 30.

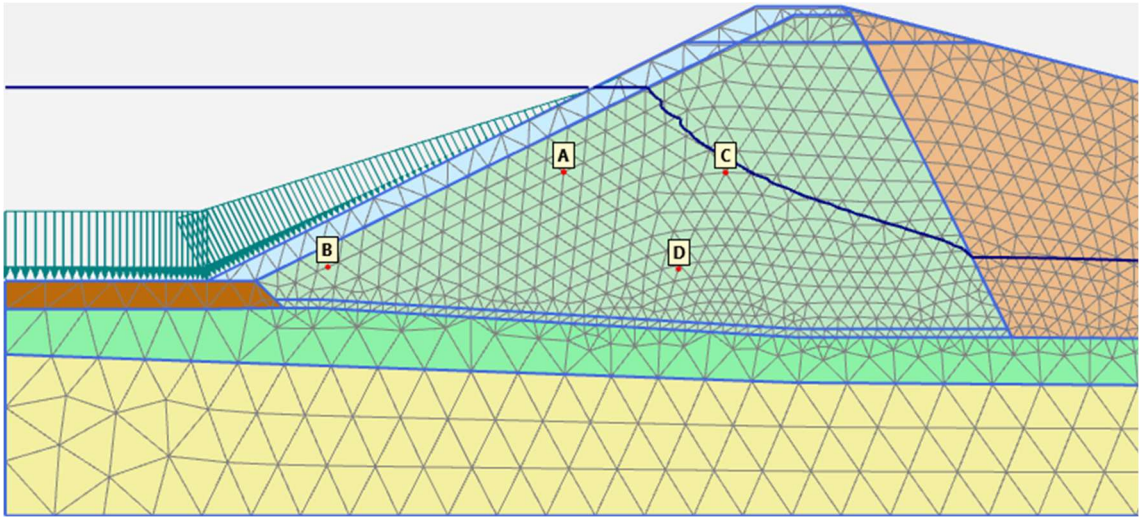

Fig. 30 Developing steady state groundwater level for filled reservoir

It can be seen that all selected nodes are located below the phreatic level inside the dam. Resulting steady state pore water pressures are shown in Tab. 9. However, considering the effect of suction increases the effective stresses in the core and the top gravel above the phreatic level. This results in a higher factor of safety. The distribution of the degree of saturation is shown in Fig. 31.

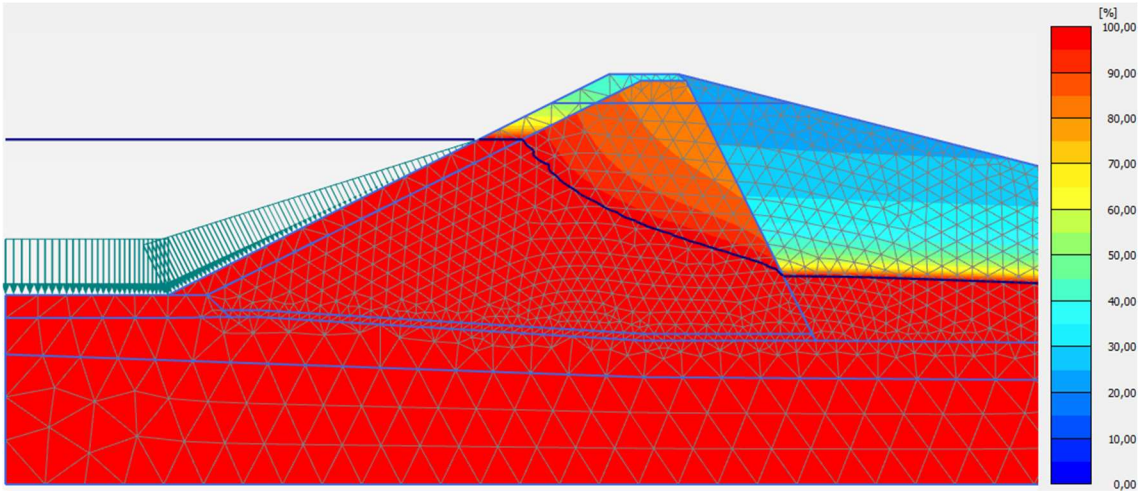

Fig. 31 Degree of saturation and steady state groundwater level with suction for filled reservoir

Tab. 9 Pore water pressures for filled reservoir

Node	Pore water pressure [kN/m²]
A	-22.24
B	-57.44
C	-3.18
D	-32.88

After the calculation of the steady state ground water level a safety analysis, using the strength reduction method, is performed to evaluate the factor of safety. The developing failure mechanisms as well as the calculated factors of safety are shown in the figures 32 and 33.

Due to the increased effective stresses, as a result of the partially saturation, also the factor of safety is increased, compared to the aforementioned analysis without any suction effects. This can be seen by the higher factors of safety.

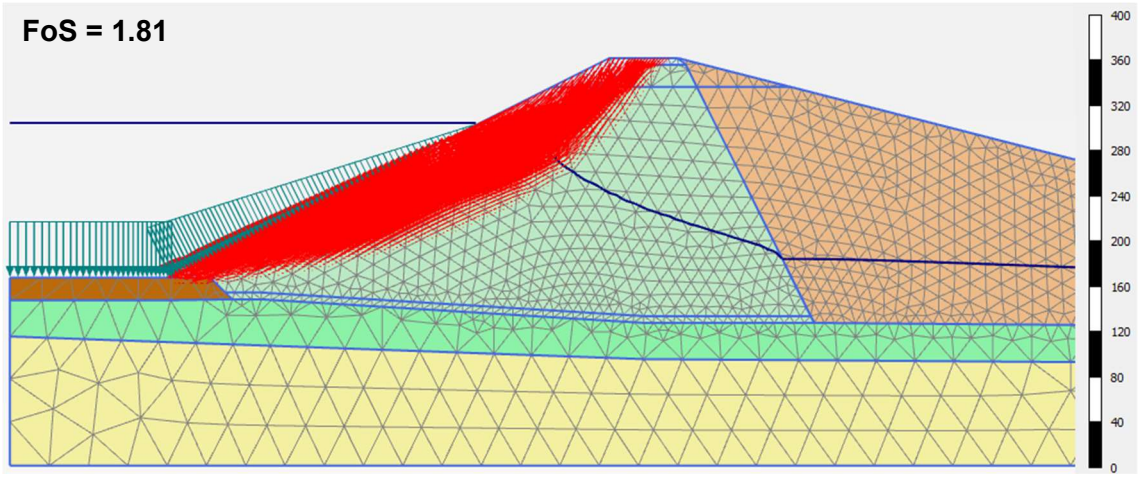

Fig. 32 Phase displacements for filled reservoir with suction after safety analysis

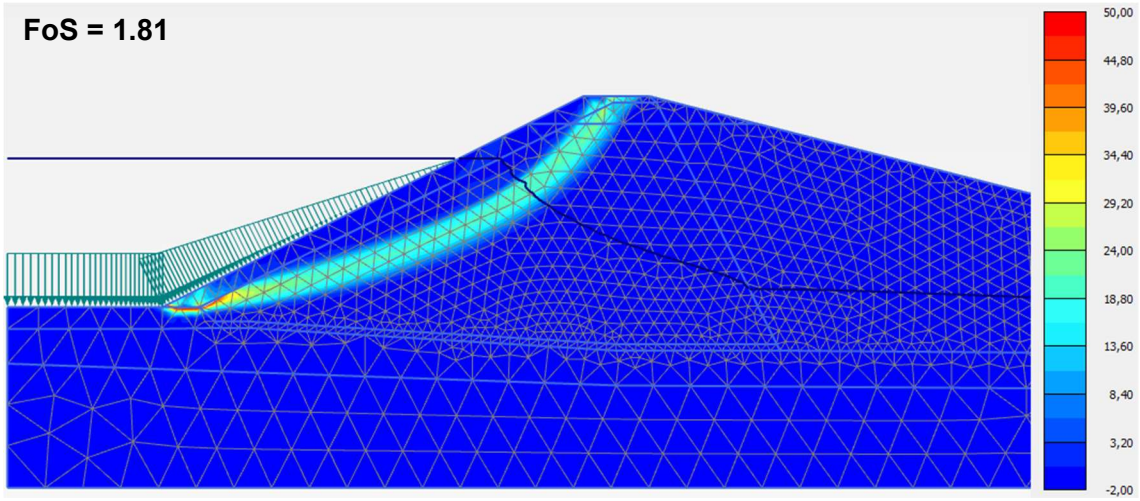

Fig. 33 Phase deviatoric strains for filled reservoir with suction after safety analysis

5.7.2 Empty reservoir

For an empty reservoir where the external water level is located at the ground surface the steady state pore water pressures and the factor of safety is determined. The developing steady state water level is shown in Fig. 34.

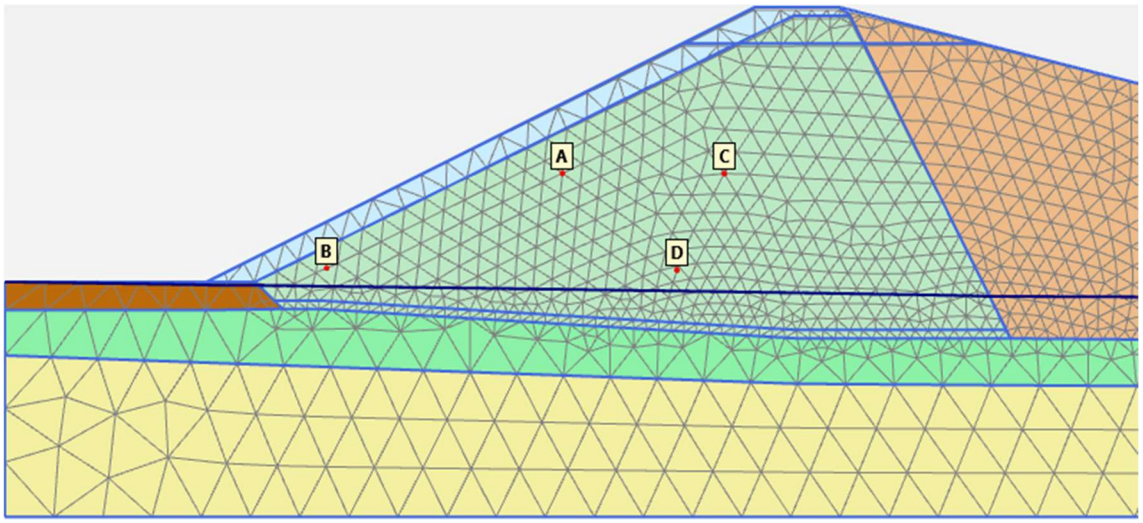

Fig. 34 Developing steady state groundwater level for empty reservoir

Considering the case of an empty reservoir all the analysed nodes are located above the phreatic level. Due to this fact and the considered partially saturated state, suction occurs in the selected nodes. The developing saturation distribution due to an empty reservoir is shown in Fig. 35. The pore water pressures in the selected nodes are shown in Tab 10.

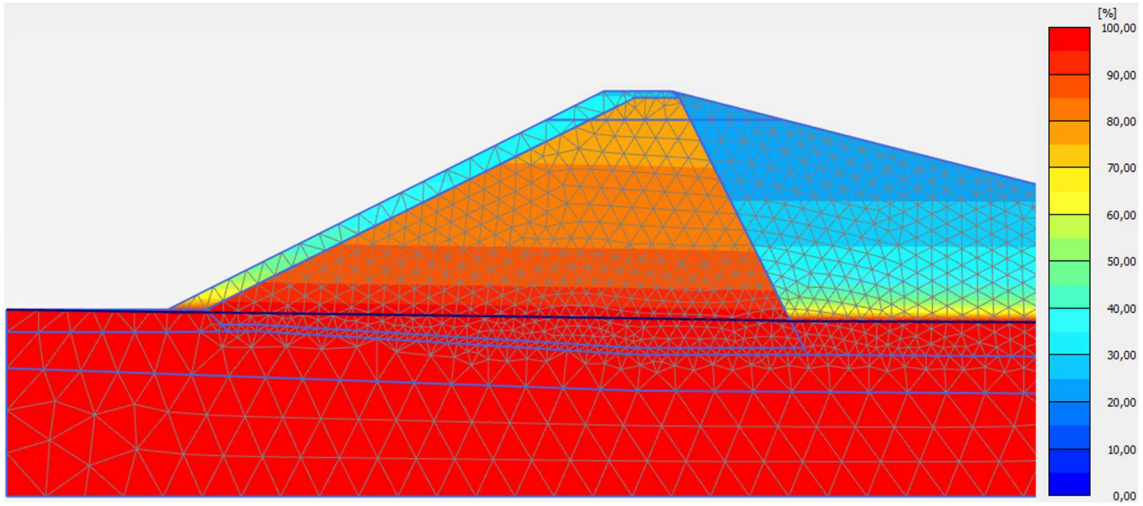

Fig. 35 Degree of saturation and steady state groundwater level with suction for empty reservoir

Tab. 10 Pore water pressure for empty reservoir

Node	Pore water pressure [kN/m²]
A	41.53
B	6.55
C	42.50
D	7.76

The performed safety analysis provides a factor of safety which is just a bit lower than for a filled reservoir although there is no stabilizing water body present. This results from the fact that the failure mechanism is different. The suctions enlarges the developing failure mechanism and it is therefore shifted towards the centre of the dam.

The displayed phase displacements (Fig. 36) show the developing failure mechanism. The factor of safety for the case of an empty reservoir is 1.73.

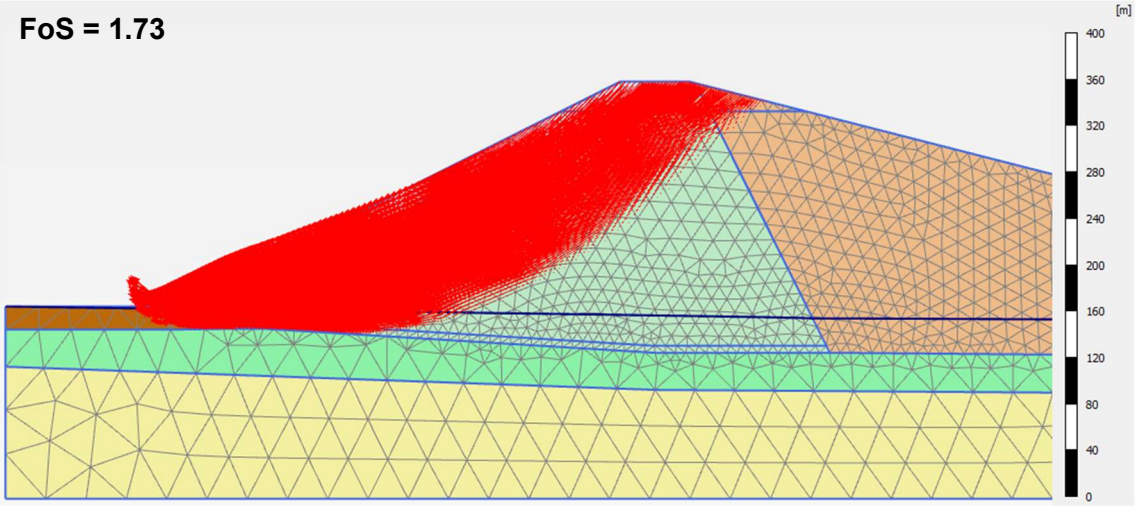

Fig. 36 Phase displacements for empty reservoir with suction after safety analysis

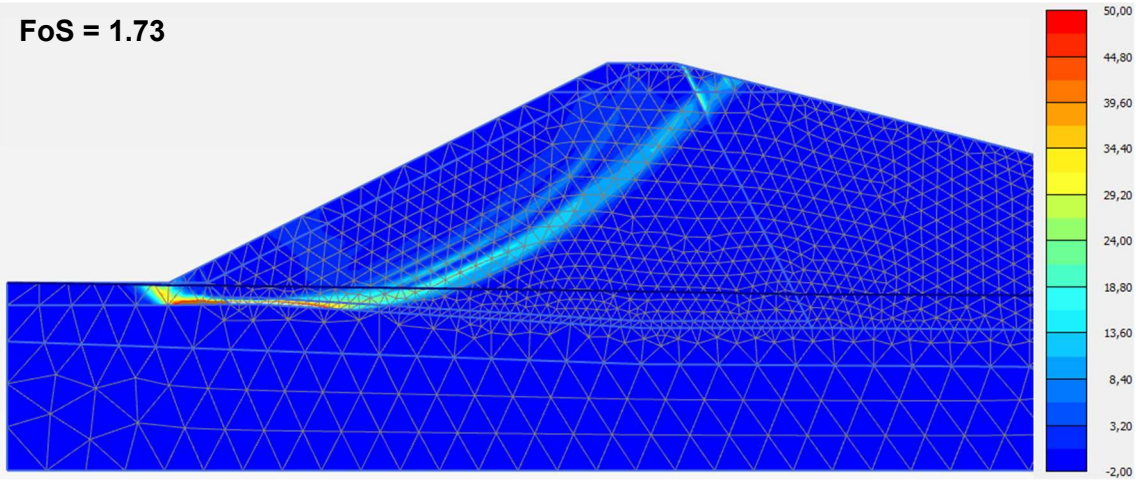

Fig. 37 Phase deviatoric strains for empty reservoir with suction after safety analysis

5.7.3 Rapid drawdown

In case of a rapid drawdown, the external water level is lowered within 18h from a height of 6.83 m above ground surface. Due to the fast lowering and the low permeable core material the internal water level remains higher than the external one (see Fig. 38 and compare Fig. 30 for initial situation). The resulting distribution of saturation after a rapid drawdown can be seen in Fig. 39.

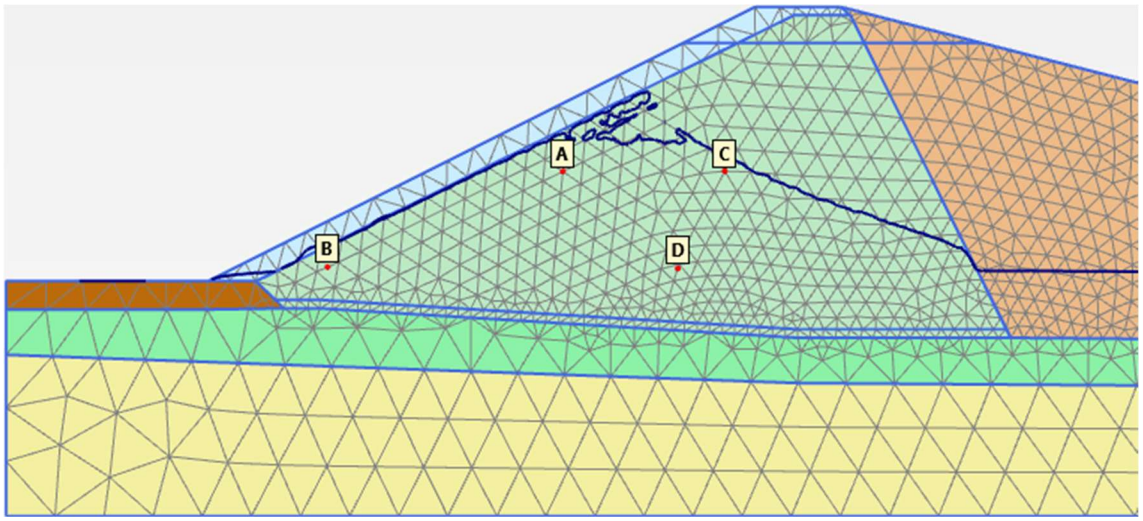

Fig. 38 Developing steady state groundwater level after rapid drawdown

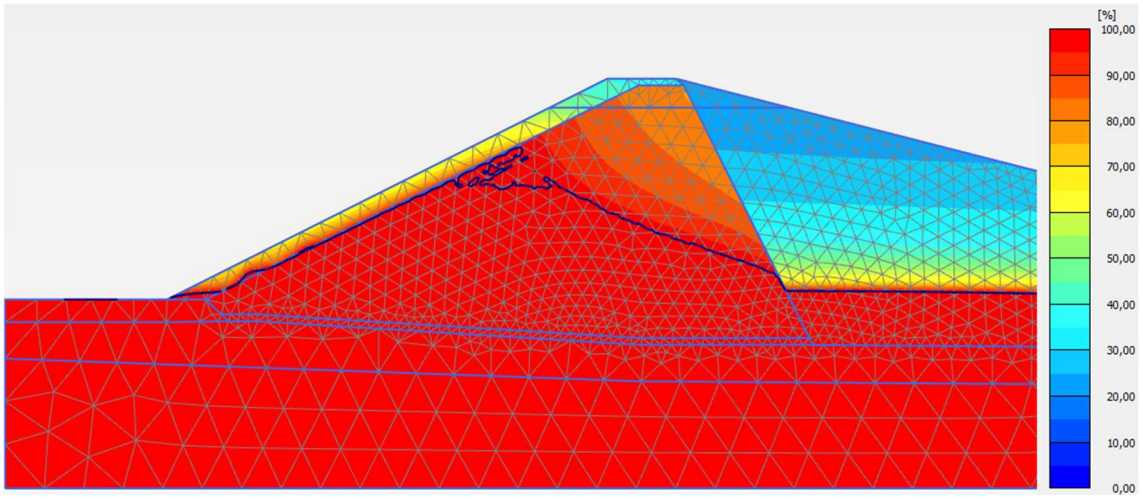

Fig. 39 Degree of saturation and steady state groundwater level with suction after rapid drawdown

Due to the change of the external water level the total stresses inside the dam change and produce excess pore water pressures. Furthermore, a hydraulic gradient from the core to the upstream side occurs because of the higher water level inside the core. The pore water pressure development during the drawdown event is shown in Fig. 40.

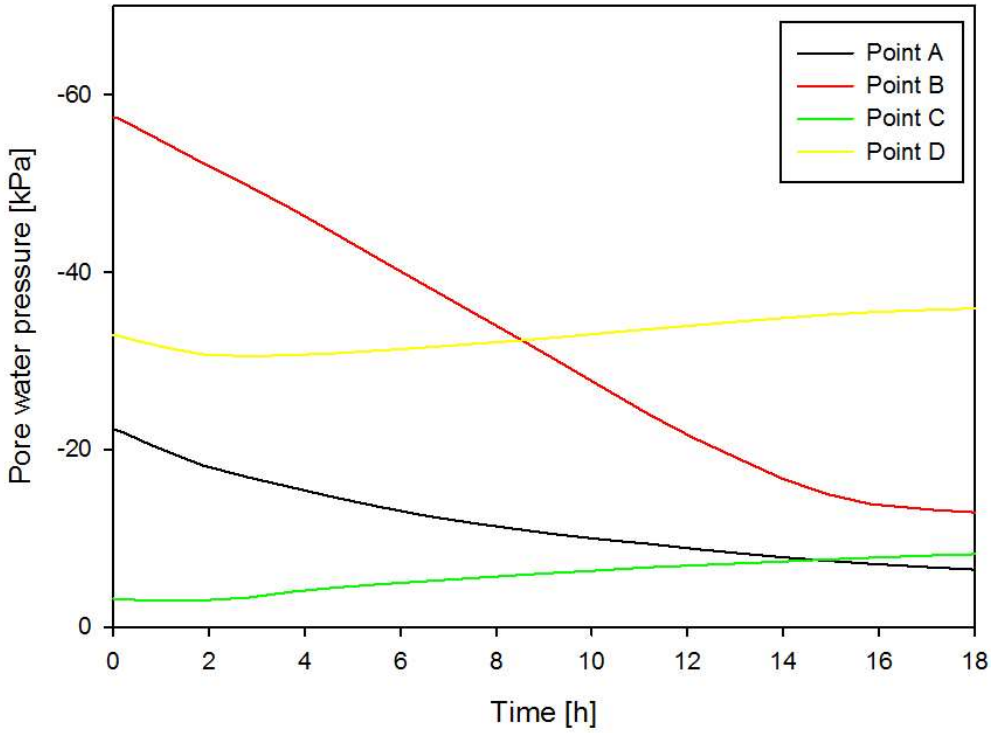

Fig. 40 Pore water pressures during rapid drawdown

It can be seen that for the nodes A and B (represented in black and red respectively) the pore water pressure decrease simultaneously with the water level change. These nodes are located in the core slightly below the high permeable top gravel.

The deformations resulting from the drawdown produce an increased pore water pressure in nodes C and D (green and yellow respectively).

The performed safety analysis for a rapid drawdown provides a factor of safety of 1.02. Compared to the FoS of the filled and the empty reservoir, this low FoS shows the significant effects of a rapid drawdown on the slope stability in case of low permeable materials.

In contrast to the analysed rapid drawdown following the principle of classical soil mechanics, a considered partially saturated state will not result in failure. Due to the considered suction, the effective stresses inside the dam are increased. Therefore, the slope is more stable. However, a higher drawdown rate may lead to slope failure. The next shown figures present the phase displacements and the phase deviatoric strains during the safety analysis. As it can be seen, a clear failure mechanism develops.

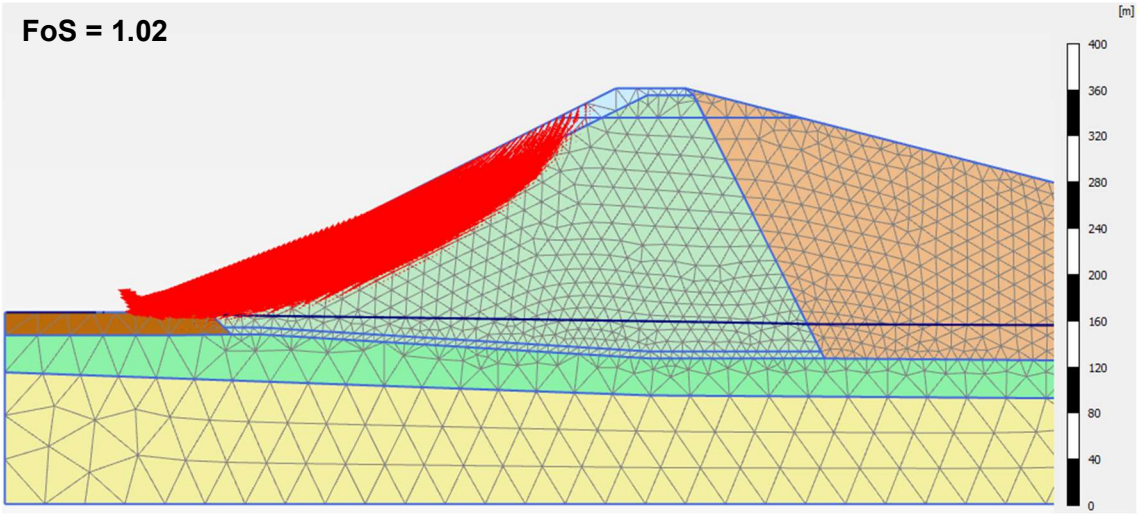

Fig. 41 Phase displacements after rapid drawdown with suction after safety analysis

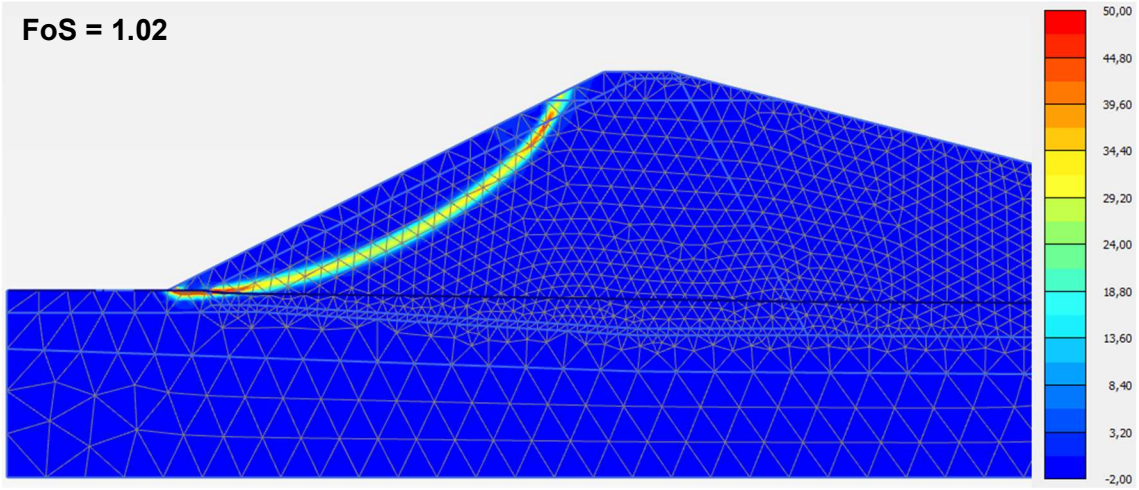

Fig. 42 Phase deviatoric strains after rapid drawdown with suction after safety analysis

5.7.4 HQ100

In this subchapter the flood event HQ100, based on the given hydrograph, is analysed and the pore water pressure development as well as the factor of safety is evaluated. First, the external water level is increased (impoundment) and afterwards decreased again (drawdown). For both scenarios, the impoundment and the subsequent drawdown, the factor of safety is computed. The time for the entire process is 25 h.

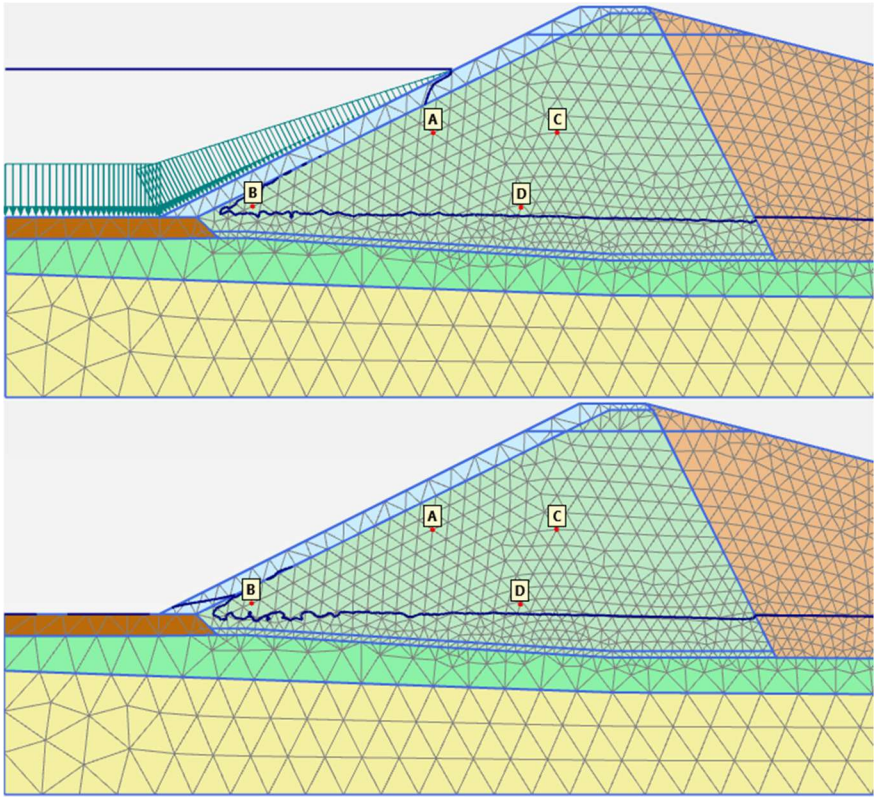

Fig. 43 Developing steady state groundwater level after a.) Impoundment and b.) Drawdown

Because the process of impoundment does not take much time and the low permeability of the core material, the water is not able to infiltrate the core as a whole. To develop a long term internal water level a longer time period with a constant high water level after impoundment would be necessary. After the drawdown the water level is almost at the same position as the initial ground water level.

The change in the external water level however, stabilizes the inclined surface and increases the resulting factor of safety. Pore water pressure development for impoundment and the following drawdown is shown in Fig. 44.

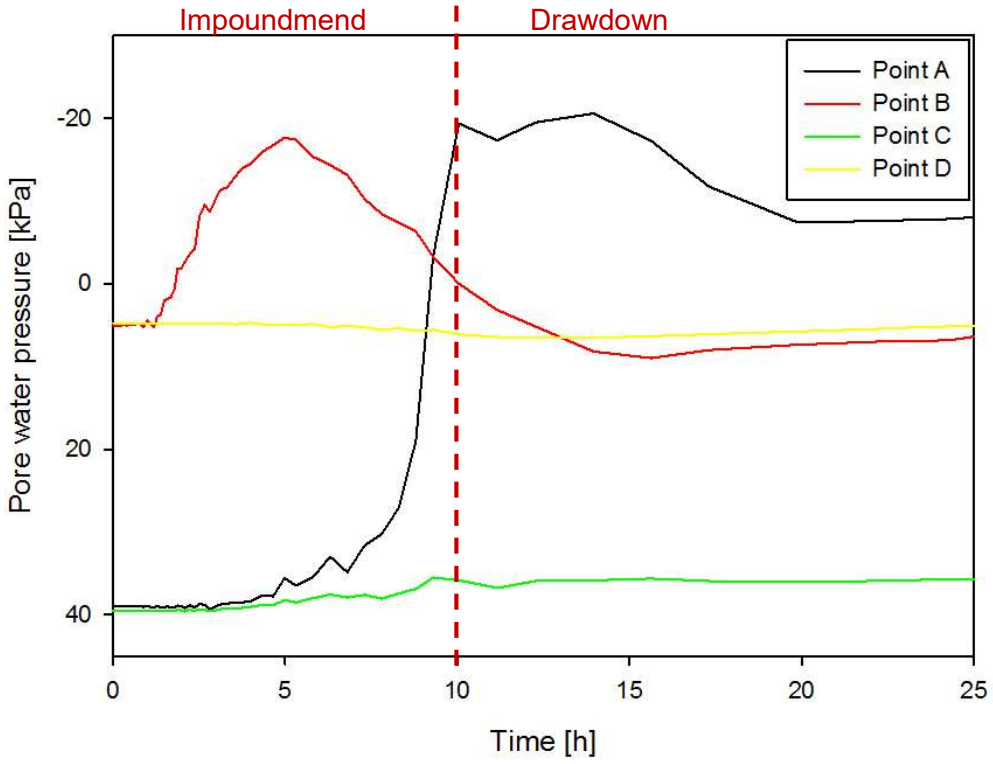

Fig. 44 Pore water pressures during HQ100

As Fig. 44 shows, for the initial conditions the phreatic level is located below the evaluated nodes, they show positive pore water pressure as suction is considered. The nodes A and B (black and red line, respectively) show the most significant increase during impoundment. Pore water pressures in node A are increased until the end of impoundment due to the rising water level. Node B shows an increase at the beginning as the rising external water level results in a change of total stresses. After a certain time (approximately 5h) water flow influences the pore water pressures and therefore the pore water pressures are decreased again.

Node D (yellow) shows no significant change in pore water pressure during HQ100 as it is located approximately in the centre of the core. The time of impoundment is too short to see significant changes as the core does not saturate. In node C (green) a small increase in pore water pressure is the result of the water level change produced due to the impoundment. The reached pore pressures remain as the drawdown happens directly after impoundment also in a short time.

Due to the separated safety analysis for the impoundment and the subsequent drawdown two safety factors are provided. After the impoundment the factor of safety results in 2.14. For the subsequent drawdown the factor of safety is 1.69.

Referred to the impoundment the increased factor of safety results from the high external water level. Furthermore, the time is too short to saturate the core, due to its low permeability. The developing failure mechanism is shown in Fig. 45. It is obvious, that the failure mechanism changes significantly, compared to a filled reservoir.

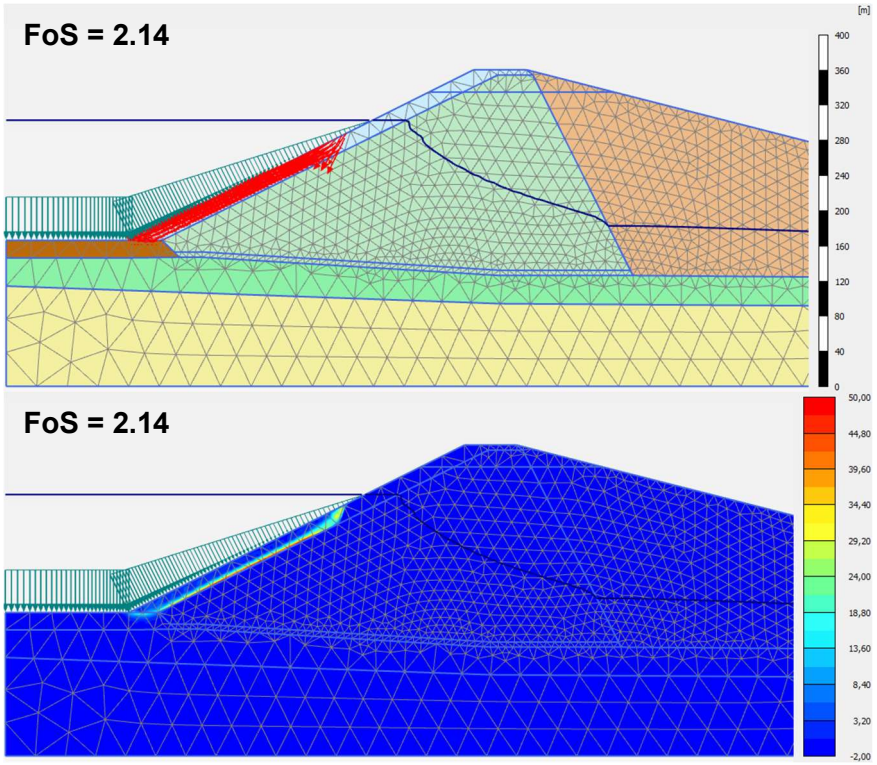

Fig. 45 a.) Phase displacements and b.) Phase deviatoric strains for impoundment with suction after safety analysis

Regarding the subsequent drawdown, the resulting factor of safety is similar to the factor of safety of the empty reservoir. The small difference in the factor of safety results from the slightly changed pore water pressure distribution. The developing failure mechanisms are shown in Fig. 46.

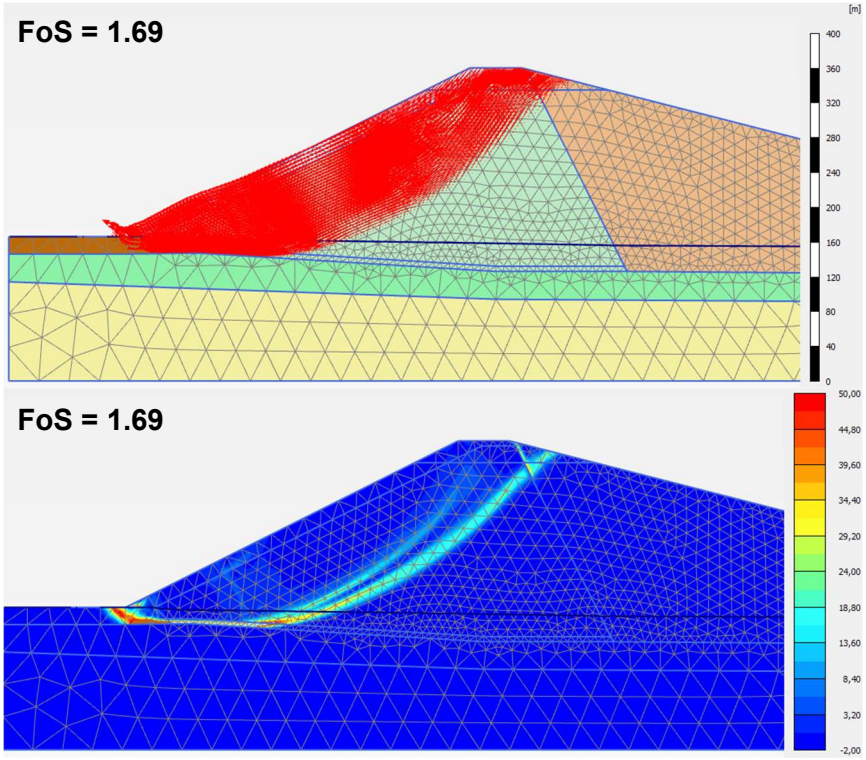

Fig. 46 a.) Phase displacements and b.) Phase deviatoric strains for subsequent drawdown with suction after safety analysis

Summarizing the results for HQ100 it can be said that for such high impoundment rates in combination with the low permeability of the core material the impoundment with the subsequent drawdown leads to no significant reduction of the slope stability.

In the following chapter the same load cases are analysed with a quasi-saturated soil water characteristic curve for the area beneath the phreatic level. Finally, the results are compared to the analyses with a conventional SWCC for the partially saturated state.

5.8 Quasi-saturated analysis

To investigate the influence of a quasi-saturated state on the pore water pressure development and on the slope stability, the soil water characteristic curves is modified according to chapter 5.4.3 (see Fig. 25). Those extended curves are applied to the low permeable materials of the core and the silt layer.

5.8.1 Filled and empty reservoir

The resulting factors of safety for a filled reservoir as well as for an empty reservoir do not differ significantly from the results of a partially saturated soil (chapter 5.7). This results from the steady state pore pressure calculation in the initial phase. The active pore water pressure differs slightly due to the difference in the degree of saturation and due to the modified soil water characteristic curve, but the pore water pressures are

similar. The difference in the pore water pressure is due to the different steady state groundwater level caused by the different permeability. Also the calculated factors of safety result in the similar values of 1.86 and 1.84 for a filled and an empty reservoir respectively. The deviation of the results for a filled reservoir is approximately 2% and for the empty reservoir the deviation is approximately 6%. The developing failure mechanisms are in fact nearly the same as it can be seen in Fig. 47.

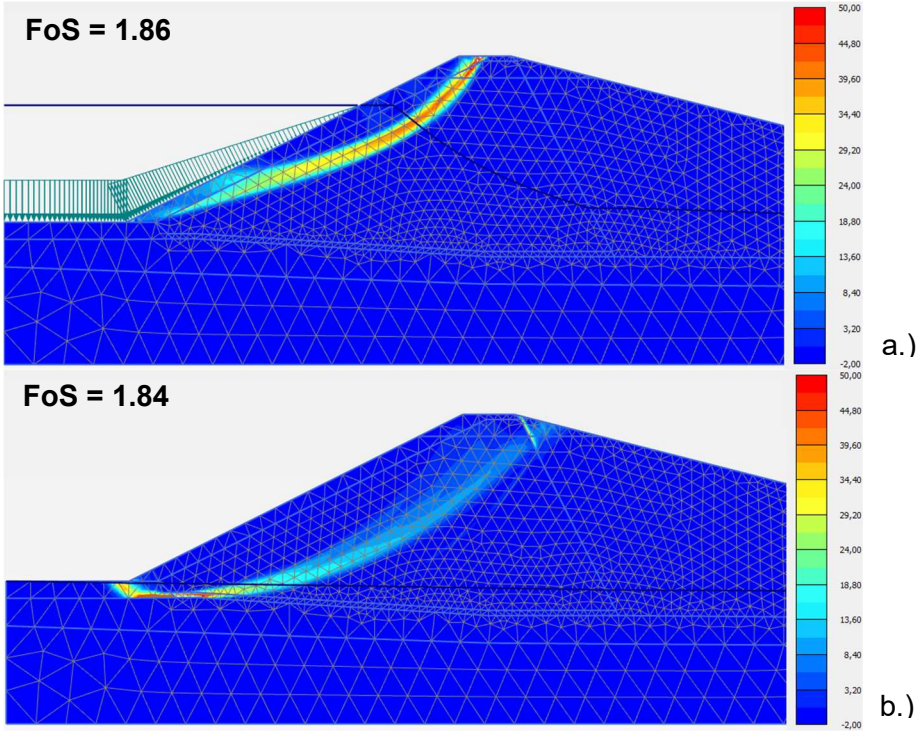

Fig. 47 Phase deviatoric strains for a.) Filled reservoir and b.) Empty reservoir considering a quasi-saturated state after safety analysis

5.8.2 Rapid drawdown

A rapid drawdown scenario results in a failure in case of a quasi-saturated state for the silt and the core material. Due to the developing high excess pore water pressure (see Fig. 49), the stability of the dam is decreased significantly. These excess pore water pressures again result from the changed load distribution between the pore fluid and the soil skeleton as described in chapter 4.3 and 4.4.

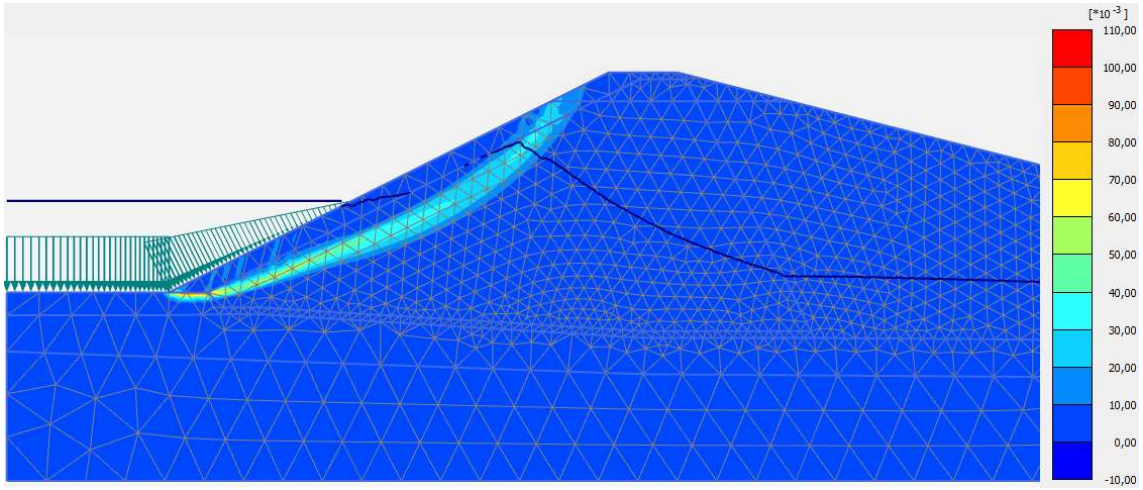

Fig. 48 Developing failure mechanism during rapid drawdown considering a quasi-saturated state due to fully coupled flow deformation analysis

The figure above shows the deviatoric strains and display clearly the developing failure mechanism during the drawdown event. It can also be seen that the soil body collapses approximately in the middle of the drawdown.

Pore pressures cannot dissipate fast enough during the drawdown and the resulting excess pore water pressure inside the core causes a failure. The shown groundwater head gives an indication about the developing excess pore water pressures (see Fig. 49).

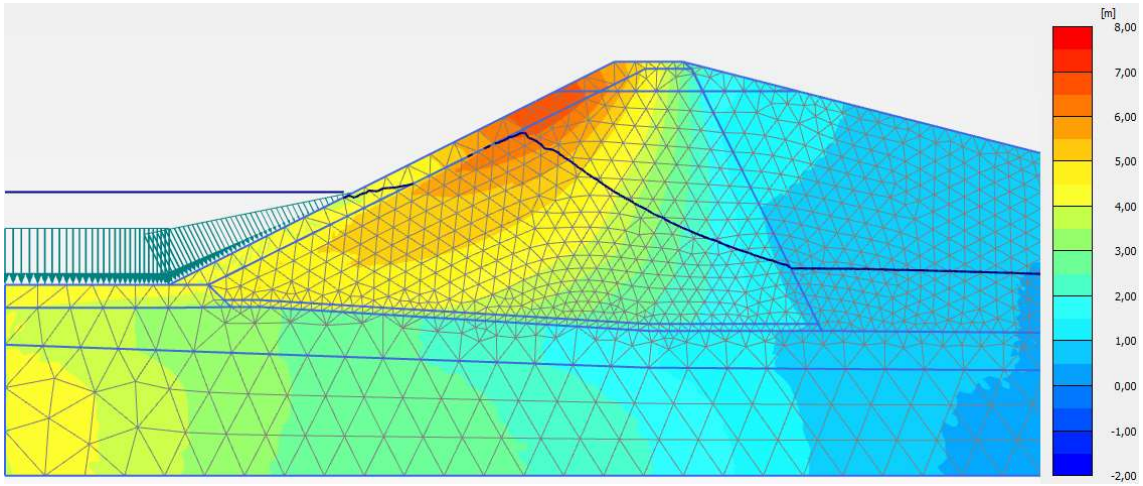

Fig. 49 Groundwater head at failure considering a quasi-saturated state during rapid drawdown

The influence of the quasi-saturation on the degree of saturation is shown in Fig. 50. To show only the quasi-saturated range, the legend of the plot is adapted. Only the quasi-saturated range is shown. The degree of saturation is increasing with depth and with increasing pore water pressure.

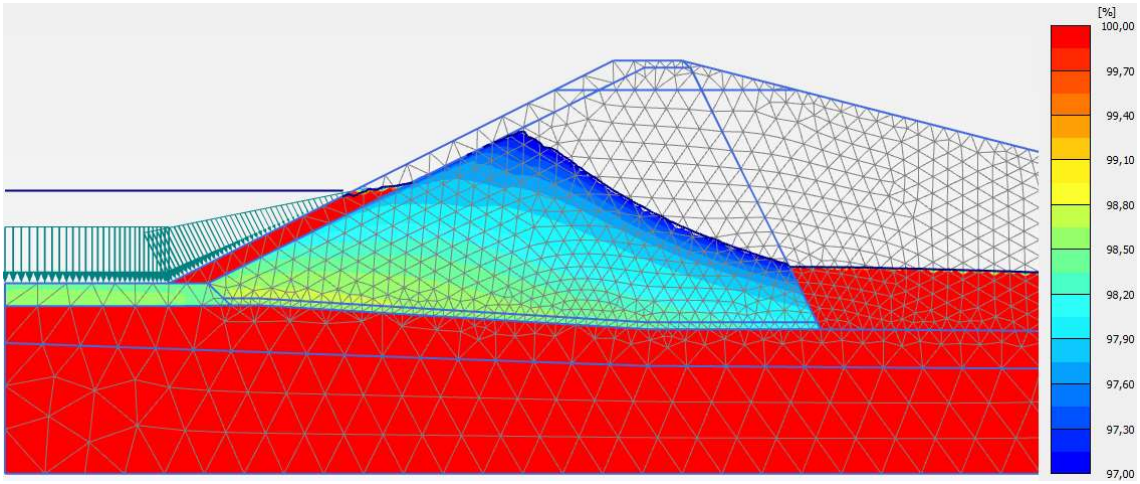

Fig. 50 Degree of saturation for the quasi-saturated range during a rapid drawdown

The produced excess pore water pressures, caused by the drawdown and the deformations, decrease slope stability significantly and lead to a collapse of the soil body. The calculation stops at M_{stage} = 0.409.

5.8.3 HQ100

Pore water pressure development and factor of safety are also analysed for HQ100 according to the hydrograph. The process of impoundment and subsequent drawdown is the same as in the partially saturated analysis.

Again, caused by the short time for the impoundment it is not possible to saturate the core. Due to the fact that the internal water level is not raised as fast as the external one, the slope experiences the stabilizing effect of the water pressure. This increases the stability of the dam. The developing internal water level after impoundment is shown in Fig. 51 a).

The effects of such a short impoundment on a subsequent drawdown are the same as aforementioned in the partially saturated analysis for a HQ100 (chapter 5.7.4)

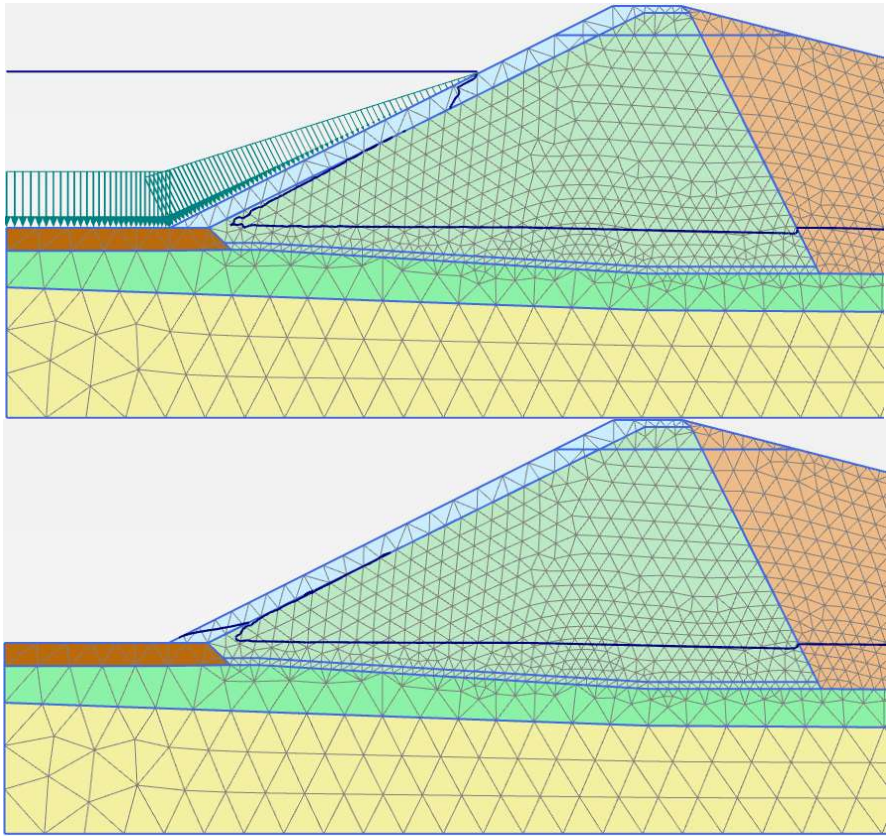

Fig. 51 Developing steady state groundwater level line after a.) Impoundment and b.) Drawdown considering a quasi-saturated state

Fig. 52 shows that due to the considered suction above the phreatic level, initial pore water pressures are positive at the beginning. In contrast to the partially saturated analysis, the pore water pressures in the nodes A and B (represented by the black and red line respectively) do not change significantly. Pore pressure in node A starts to increase as the phreatic level increases. Right before the drawdown starts pore pressures start to dissipate again as the water starts saturating the dam. In node B whereas pore pressures start to increase directly with the start of the impoundment. Once the water starts to infiltrate the core however, pore pressures are decreased again. After drawdown also in node B a small amount of excess pore pressure develops due to the subsequent drawdown.

Like in the partially saturated analysis, nodes C and D (green and yellow line) show no significant change in pore water pressures as they are located far inside the dam. To see an influence on pore water pressure development a longer steady state after impoundment would be necessary.

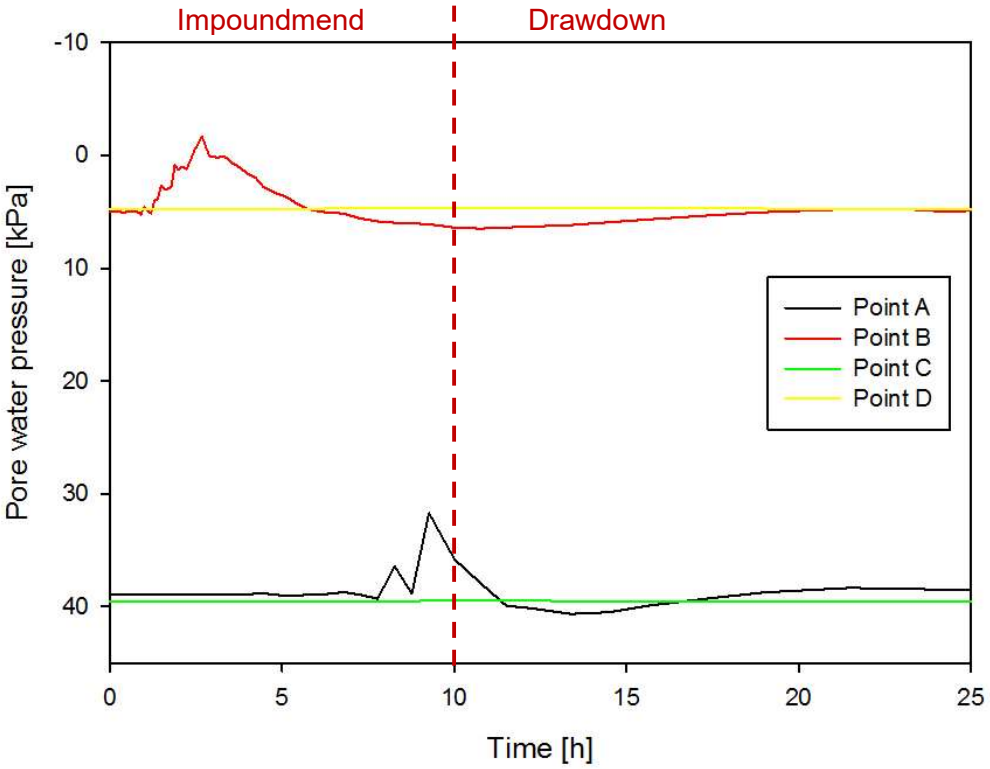

Fig. 52 Pore water pressures during HQ100 considering a quasi-saturated state

Again, the factor of safety for impoundment arises from the increase of the external water level. Due to the rising external water level and the low permeable core, the slope gets stabilized on the surface. The developing failure mechanism as well as the factor of safety are shown in Fig. 53.

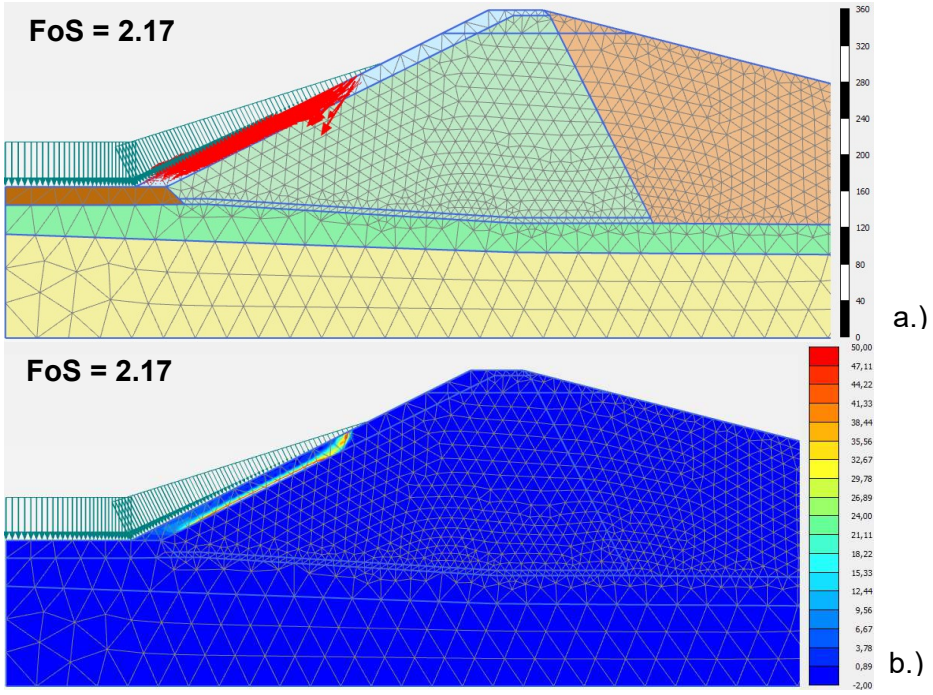

Fig. 53 a.) Phase displacements and b.) Phase deviatoric strains for impoundment considering a quasi-saturated state after safety analysis

For the subsequent drawdown the developing failure mechanism is located in the area of the slope toe, due to the remaining internal water level caused by the impoundment. Although, the impoundment was within a short time the internal water level rises, high pore pressures are produced at the dam toe. These excess pore water pressures are caused by the quasi-saturated state of the silt layer.

The developing failure mechanism caused by the subsequent drawdown is shown with the phase displacements and deviatoric strains in Fig. 54 a.) and b.).

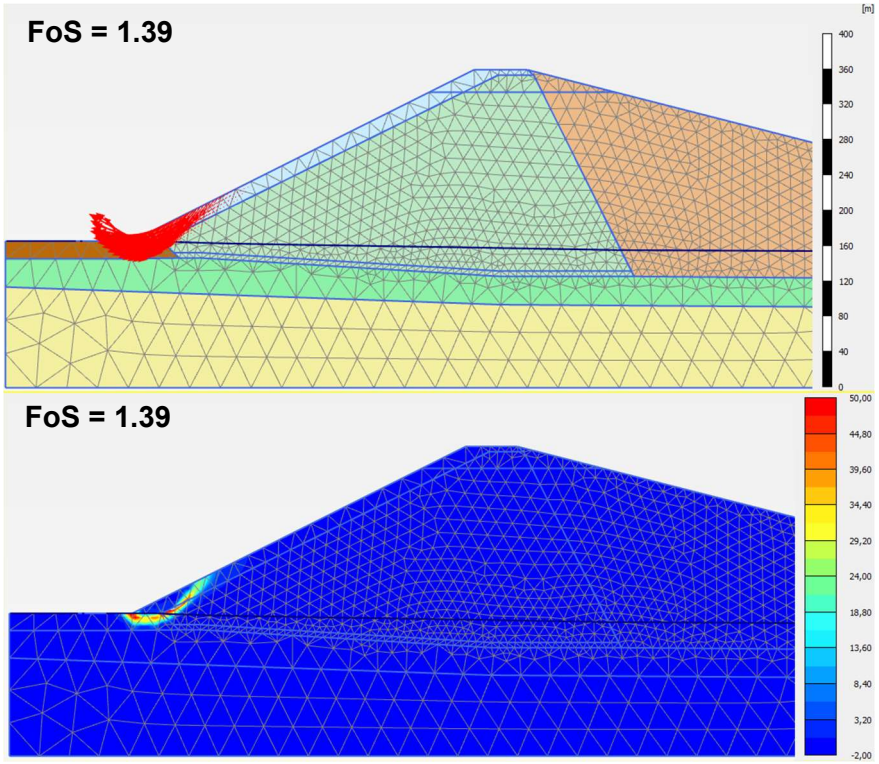

Fig. 54 a.) Phase displacements and b.) Phase deviatoric strains for subsequent drawdown considering a quasi-saturated state after safety analysis

Also in case of a quasi-saturated state it can be summarised that the impoundment as well as the drawdown rate of the HQ100 are too low to show significant influences on pore water pressure development. However, due to the short rates for the impoundment and the drawdown there is no significant reduction of the slope stability.

5.8.4 Comparison of the results for the different states of saturation

As the results for the different states of saturation show significant differences concerning the factors of safety and the developing failure mechanisms, they are compared in the following. (see Fig. 55)

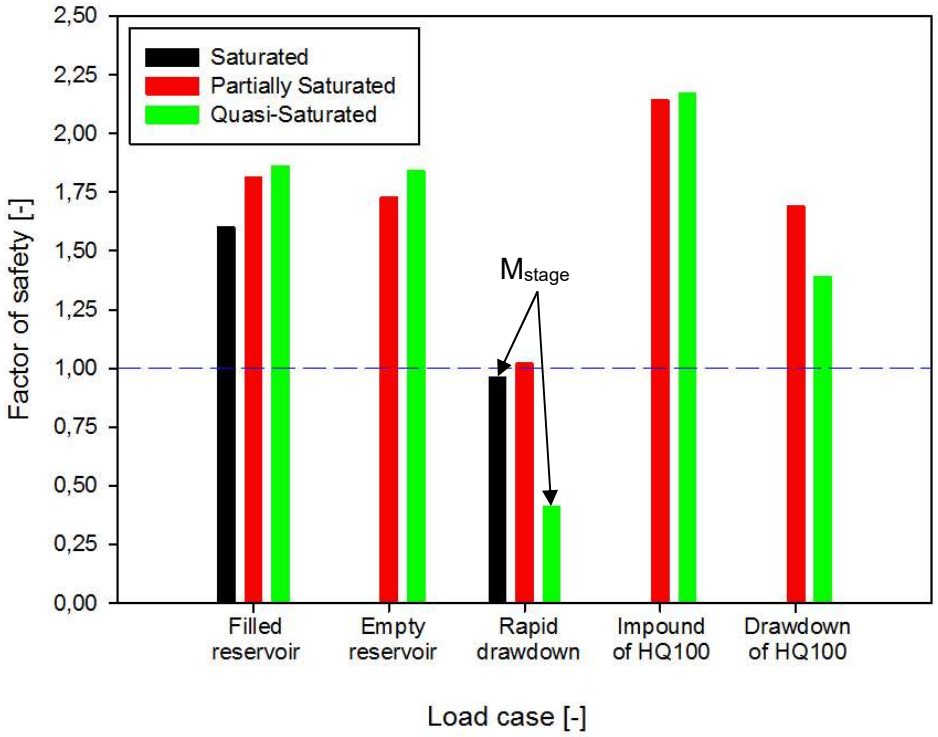

Fig. 55 Comparison of the calculated factors of safety for all load cases and states of saturation

The black bars represent the saturated analyses (following the principle of classical soil mechanics). As the load case of a rapid drawdown scenario failed, no value for the factor of safety could be determined so the value for M_{stage} is plotted in this case. Furthermore, the classical analysis was only performed for a filled reservoir and a rapid drawdown. The red and green bars represent the partially saturated analyses (considered suction above the phreatic level) and the quasi-saturated analysis (entrapped air below the phreatic level) respectively. It can be seen that for the steady state cases (filled and empty reservoir) as well as for the impoundment of HQ100 the quasi-saturated analysis provides higher factors of safety. Regarding the steady state load cases this results from the entrapped air below the phreatic level which influences the permeability (and so the developing internal groundwater level) and the degree of saturation. Only in case of the drawdown after HQ100 the factor of safety is lower when a quasi-saturated state is considered. This results from the developing excess pore water pressures caused by the quasi-saturation after lowering the external water level. Regarding the rapid drawdown scenario, a considered quasi-saturated state leads to a failure of the dam again caused by developing excess pore water pressures. In this case also M_{stage} is plotted.

As already discussed, the Skempton *B* coefficient governs the load distribution between pore fluid and soil skeleton. B defines the percentage of the load which is transferred to the water and the complement (B-1) is the part which is transferred to the soil skeleton

and produces the excess pore water pressure. So, in case of hydraulic unloading, like in the rapid drawdown and the drawdown after HQ100, excess pore pressure are the result.

For a better comparison of the pore water pressure situation after a rapid drawdown considering the different states of saturation, the ground water heads are shown in the following figures with contour. These contour plots show the results of a partially saturated and a quasi-saturated state.

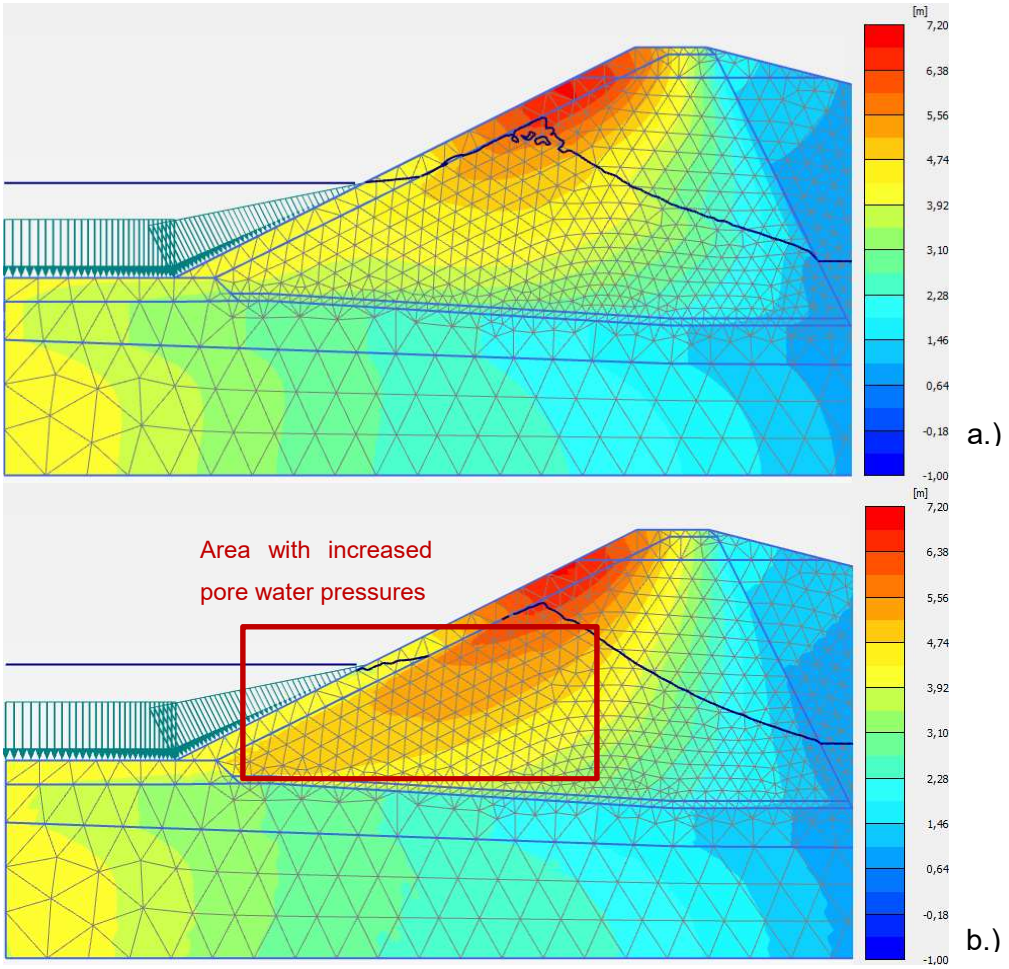

Fig. 56 Groundwater head for rapid drawdown for a.) Partially and b.) Quasi-saturated due to fully coupled flow deformation analysis

To get comparable figures, the groundwater heads are shown for the same water level, which is governed by the quasi-saturated drawdown as it fails after approximately half of the drawdown.

As Fig. 56 shows, the difference in the groundwater head is significant. Due to the fast lowering the remaining groundwater head in the core stays high and excess pore water pressures are produced, especially in the quasi-saturated case. The high remaining groundwater head inside the dam leads to failure in case of quasi-saturation. In case of

partially saturation a rapid drawdown indeed does not lead to a failure of the dam, but when the drawdown rate will be higher failure may also occur in this case.

6 Conclusion and outlook

In summary, it can be said that entrapped air and thereof a quasi-saturated state has a significant influence on the developing pore pressures in case of a change of the external water level. By influencing the pore water pressure development, also the stability of the slope is significantly influenced.

Just a small amount of entrapped air in the soil increases the compressibility of the pore fluid and as a consequence a development of excess pore water pressures could be the case. Due to the resulting deformations caused by a quasi-saturated states those excess pore water pressures can be increased even more.

The parameters like soil stiffness and permeability as well as the present degree of saturation govern the pore water pressure development in case of hydraulic load change. They should be estimated as accurate as possible for numerical analyses in order to obtain reliable results. Also, the velocity of the water level change plays a major role (as it can be seen in chapter 4).

To get a better understanding of pore water pressure development in quasi-saturated soil, it is of advantage to fit numerical analysis with in situ data. Therefore in known landslides, or creeping slopes as well as on existing flood retention basins, measurement devices could be implemented to measure pore water pressures. Also laboratory tests to determine the degree of saturation or soil permeability could be made. The obtained results can then be compared using finite elements and the insight gained can be applied to future projects.

7 Literature

Alonso, E., & Pinyol, N. (2009). Slope stability under rapid drawdown conditions. *Italian Workshop on Landslides.* Naples, Italy.

Ausweger, G. M., & Schweiger, H. F. (2016). Numerical study on the influence of entrapped air bubbles on the time-dependent pore pressure distribution in soils due to external changes in water level. In: P. Delage, Y.-J. Cui, S. Ghabezloo, j.-M. Pereira, & A.-M. Tang, *Proceedings of the 3rd European Conference on Unsaturated Soils.* Paris.

Black, D. K., & Lee, K. L. (1973). Saturating laboratory samples by back pressure. *Journal of the Soil Mechanics and Foundations Division, ASCE, Vol. 99, No. SM1*.

Boutonnier, L. (2010). Coefficient B, Consolidation, and Swelling in Fine Soils Near Saturation in Engineering Practice. In: L. Laloui, *Mechanics of Unsaturated Geomaterials.* Great Britain and the United States: ISTE Ltd. and John Wiley & Sons, Inc.

Brinkgreve, R. B. (2016). *Plaxis 2D 2016 Manual.* The Netherlands.

Faybishenko, B. A. (1995). Hydraulic behavior of quasi-saturated soils in the presence of entrapped air: Laboratory experiments. *Water Resources Research, Vol. 31*, (p. 2421).

Galavi, V. (2010). *Groundwater flow, fully coupled flow deformation and undrained analysis in Plaxis2D and 3D.*

Köhler, H.-J., & Montenegro, H. (2005). Investigations regarding soils below phreatic surface as unsaturated porous media. *Federal Waterways Engineering and Research Institute (BAW).* Karlsruhe, Deutschland.

Montenegro, H., Stelzer, O., & Odenwald, B. (2015). Parameter study on the influence of entrapped gas bubbles in groundwater on pore water pressure and effective stress following static loading or water level changes. *BAW Mitteilungen*.

Muth, W. (2001). *Hochwasserrückehaltebecken: Planung, Bau und Betrieb.* Ehningen bei Böblingen: Expert-Verlag.

Odenwald, B., Hekel, U., & Thormann, H. (2009). Grundwasserströmung - Grundwasserhaltung. In K. J. Witt, *Grundbau- Taschenbuch Teil 2: Geotechnische Verfahren* (pp. 485 - 652). Berlin, Deutschland: Verlag für Architektur und technische Wissenschaften GmbH & Co. KG.

Skempton, A. W. (1954). *The pore pressure coefficients A and B.* Géotechnique.

Technical University of Munich, Center of Geotechnics. (2016). *Chair of Soil Mechanics and Foundation Engineering, Rock Mechanics and Tunneling.* Retrieved from Technical University of Munich: https://www.gb.bgu.tum.de/fileadmin/w00bpk/www/Lehre/Studienunterlagen/Vorlesungsskript/11_vorlg-h.pdf